| | | | | | |
|---|---|---|---|---|---|
| 21) 大矢亜紀, 中原　徹, 野村　渉, 大庭　賢二, 田中智博, 橋本知恵, 鳴海哲夫,村上　努, 山本直樹,玉村　啓和. | HIV-gp41 の三量体構造に特異的な中和抗体を誘導する人工抗原ペプチド. | 第 28 回メディシナルケミストリーシンポジウム講演要旨集 | | 246-247 | 2009 |
| 22) 橋本知恵, 野村　渉, 田中智博,中原　徹, 鳴海哲夫, 大庭賢二, 村上努, 山本直樹, 玉村啓和. | エイズワクチンを指向した宿主受容体CXCR4由来抗原分子の創製. | 日本薬学会第 130 年会要旨集 | | 28TG -am05 | 2010 |
| 23) 田中智博, 野村　渉, 鳴海哲夫,玉村啓和. | 二価型 CXCR4 リガンドの創製と二量体構造解析への応用. | 日本薬学会第 130 年会要旨集 | | 28TG -am06 | 2010 |
| 24) 大橋南美, 野村　渉, 鳴海哲夫,奥田善章, 伊倉貞吉, 伊藤暢聡, 吉田清嗣, Lewin NE, Blumberg PM, 玉村啓和. | 蛍光を用いた PKC リガンド結合評価法の開発. | 日本薬学会第 130 年会要旨集 | | 28TG -am08 | 2010 |
| 25) 鳴海哲夫, 清家俊輔, 野村　渉, 玉村啓和. | 新規アミド等価体クロロアルケン型ジペプチドイソスターの合成研究. | 日本薬学会第 130 年会要旨集 | | 29TF -am03 | 2010 |
| 26) 鳴海哲夫, 落合千裕, 山田裕子, 吉村和久, 原田恵嘉, 大橋南美, 野村　渉, 松下修三, 玉村啓和. | HIV-1 外被タンパク質 gp120 の構造変化誘起を指向した低分子 CD4 ミミックの構造活性相関研究. | 日本薬学会第 130 年会要旨集 | | 29TG -am05 | 2010 |
| 27) 野村　渉, 中原　徹, 大矢亜紀, 大庭賢二, 田中智博, 橋本知恵, 鳴海哲夫, 村上　努, 山本直樹, 玉村啓和. | 合成人工抗原ペプチドによる HIV-gp41 の三量体構造を認識する抗体の誘導. | 日本薬学会第 130 年会要旨集 | | 29TK -am05Q | 2010 |
| 28) 増田朱美, 野村　渉, 大庭賢二, 奥田　毅, Barbas,C.F.,III, 山本直樹, 玉村啓和. | 配列特異的 DNA 組換え酵素における DNA 結合親和性が及ぼす組み換え反応効率への影響. | 日本薬学会第 130 年会要旨集 | | 28SH -am15 | 2010 |

Research Article

Journal of PeptideScience

Received: 4 April 2009 Revised: 11 June 2009 Accepted: 15 June 2009 Published online in Wiley Interscience: 11 August 2009

(www.interscience.com) DOI 10.1002/psc.1161

# Synthesis of protein kinase Cδ C1b domain by native chemical ligation methodology and characterization of its folding and ligand binding‡

**Nami Ohashi,[a] Wataru Nomura,[a]* Mai Kato,[a] Tetsuo Narumi,[a] Nancy E. Lewin,[b] Peter M. Blumberg[b] and Hirokazu Tamamura[a]***

**The C1b domain of protein kinase Cδ (PKCδ), a potent receptor for ligands such as diacylglycerol and phorbol esters, was synthesized by utilizing native chemical ligation. With this synthetic strategy, the domain was efficiently constructed and shown to have high affinity ligand binding and correct folding. The C1b domain has been utilized for the development of novel ligands for the control of phosphorylation by PKC family members. This strategy will pave the way for the efficient construction of C1b domains modified with fluorescent dyes, biotin, etc. Copyright © 2009 European Peptide Society and John Wiley & Sons, Ltd.**

*Supporting information may be found in the online version of this article*

**Keywords:** protein kinase C; native chemical ligation; C1b domain; ligand binding

## Introduction

Protein kinase C (PKC) isoforms are serine/threonine protein kinases which play a pivotal role in physiological responses to growth factors, oxidative stress, and tumor promoters. These responses regulate numerous cellular processes [1,2], including proliferation [3], differentiation [4], migration [5], and apoptosis [6,7]. Under physiological conditions, signal transduction through PKC is triggered by the interaction between diacylglycerol (DAG), a lipid second messenger, and the C1 domains of PKC. The C1 domain is well conserved within the PKC superfamily, forming a zinc finger structure into which the DAG or phorbol ester inserts. Ten PKC isoforms have been described, among which PKCδ, a member of the novel PKC subfamily, is DAG/phorbol ester-dependent but calcium-insensitive. Development of ligands with high specificity for PKC isozymes has been a critical issue [8–10]. Considerable attention has been directed at the development of inhibitors of PKC isoforms; however, for PKCδ, activators have a therapeutic rationale. For example, PKCδ is growth-inhibitory in NIH3T3 cells, whereas PKCα and PKCε are growth-stimulatory [10]. Thus, complementary therapeutic strategies are to inhibit a specific PKC isoform or to stimulate an antagonistic isoform. For this latter approach, activators selective for different isoforms are needed.

For the development of isozyme-specific ligands, the C1b domain provides a robust platform for binding analyses. Although bacterial expression of cloned C1b domain affords ample material, preparation of the C1b domain by synthetic methods would greatly enhance its ability to be manipulated, such as by labeling with fluorescent dyes or biotin. However, synthesis of the C1b domain by standard SPPS is problematic on account of its size (~50 amino acids), although its synthesis by a stepwise condensation method has proven possible [11]. In this study, we applied native chemical ligation (NCL) methodology [12,13] to an efficient synthesis of the PKCδ C1b (δC1b) domain (Scheme 1).

## Materials and Methods

### Preparation of amino acid-loaded 2-chlorotrityl resin

2-Chlorotrityl chloride resin (100–200 mesh polystyrene, 1% DVB, 1.4 meq/g, 1.4 mmol) (Novabiochem) was treated with Fmoc-His(Trt)-OH (0.63 mmol) and *N,N*-diisopropylethylamine (DIPEA) (2.25 mmol) in dry DCM (10 ml) for 1 h. The resin was dried *in vacuo* after washing with dry DCM. The loading was determined by measuring UV absorption at 301 nm of the piperidine-treated Fmoc-His(Trt)-(2-Cl)Trt-resin (0.32 meq/g). Unreacted chloride was capped by treatment with MeOH (1 ml), DCM (10 ml), and DIPEA (574 µl, 3.3 mmol) for 15 min.

### Synthesis of peptide thioester δC1b(231–246)

The peptide chain was manually constructed using Fmoc-based solid-phase synthesis on Fmoc-His(Trt)-(2-Cl)Trt-resin with capping

* *Correspondence to: Wataru Nomura and Hirokazu Tamamura, Institute of Biomaterials and Bioengineering, Tokyo Medical and Dental University, 2-3-10 Kandasurugadai, Chiyoda-ku, Tokyo 101-0062, Japan. E-mail: tamamura.mr@tmd.ac.jp; nomura.mr@tmd.ac.jp*

a *Institute of Biomaterials and Bioengineering, Tokyo Medical and Dental University, 2-3-10 Kandasurugadai, Chiyoda-ku, Tokyo 101-0062, Japan*

b *Laboratory of Cancer Biology and Genetics, Center for Cancer Research, National Cancer Institute, National Institutes of Health, Bethesda, MA 20892, USA*

‡ *Dedicated to Dr. Victor E. Marquez on the occasion of his 65th birthday.*

Journal of PeptideScience

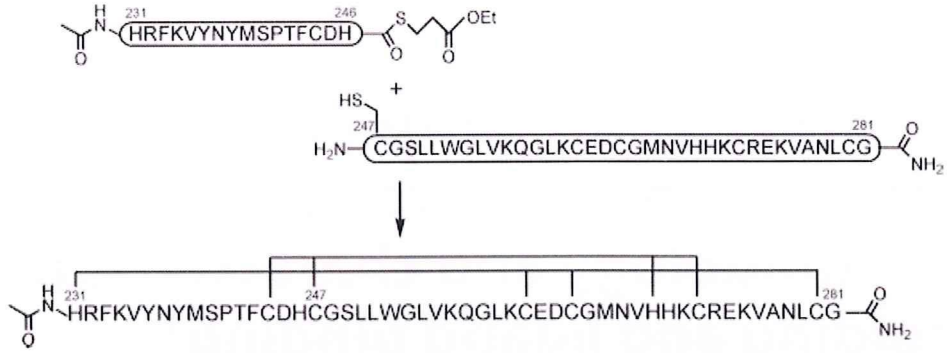


**Scheme 1.** Process of NCL methodology and the sequence of synthesized δ C1b domain. The amino acid residues involved in chelation of zinc ions are grouped by lines.

(0.05 mmol scale). Fmoc-protected amino acid derivatives (5 equiv) were successively condensed using 1,3-diisopropylcarbodiimide (DIPCI) (5 equiv) in the presence of HOBt·$H_2O$ (5 equiv) in DMF (2 ml) (90 min treatment). The following side-chain protecting groups were used: Boc for Lys, Pbf for Arg, $OBu^t$ for Asp, Trt for Asn, Cys, and His, $Bu^t$ for Ser, Thr, and Tyr. The Fmoc group was deprotected with 20% piperidine in DMF (2 ml) for 15 min. After the final Fmoc deprotection, the peptide was acetylated in the mixture of $Ac_2O$–DMF–pyridine (1 : 4 : 1, v/v, 3 ml). The yield of the resulting protected peptide resin was 335 mg. The resulting protected δC1b(231–246) was cleaved from the resin with TFE–AcOH–DCM (1 : 1 : 3, v/v, 15 ml) (2 h treatment), and thioesterified with ethyl mercaptopropionate (20 equiv), HOBt·$H_2O$ (10 equiv), and 1-(3-dimethylaminopropyl)-3-ethylcarboiimide (EDCI)·HCl (10 equiv) in DMF (1 ml) (0 °C, 2 h). Subsequently, the peptide was deprotected with TFA–thioanisole–*m*-cresol–triisopropylsilane (TIS) (89 : 7.5 : 2.5 : 1, v/v, 5 ml) (90 min treatment). After cleavage and deprotection, the crude product was precipitated and washed three times with cold diethyl ether, then purified by RP-HPLC (column: COSMOSIL $_5C_{18}$ AR-II, 10 × 250 mm).

### Synthesis of peptide fragment δC1b(247–281)

The peptide chain was manually constructed using Fmoc-based solid-phase synthesis on NovaSyn TGR-resin (0.26 meq/g, 0.1 mmol scale). Fmoc-protected amino acid derivatives (5 equiv) were successively condensed using DIPCI (5 equiv) in the presence of HOBt·$H_2O$ (5 equiv) in DMF (4 ml) (90 min treatment). The side-chain protecting groups were used as for the synthesis of δC1b(231–246). Additionally, Trt and $OBu^t$ were used for Gln and Glu, respectively. The yield of the resulting protected peptide resin was 920 mg. Protected δC1b(247–281) was cleavaged and deprotected with TFA–thioanisole–*m*-cresol–TIS (89 : 7.5 : 2.5 : 1, v/v, 10 ml) (90 min treatment). The purification procedure was the same as in the synthesis of δC1b(231–246).

### Native chemical ligation

The thioester peptide (δC1b(231–246): 2.9 mg, 1.3 μmol), the *N*-terminal Cys peptide (δC1b(247–281): 4.9 mg, 1.3 μmol), and tris(2-carboxyethyl)phosphine hydrochloride (3 mg, 13 μmol) were dissolved in 1.5 ml of 6 M guanidine hydrochloride, 2 mM EDTA, and 0.1 M sodium phosphate at pH 8.5. The addition of 4% thiophenol promoted the conversion of the less reactive 2-mercaptopropionate thioester to the more reactive phenyl-α-thioester and started the ligation reaction [13,14]. After incubation at 37 °C under $N_2$ atmosphere, the reaction mixture was analyzed by analytical RP-HPLC (column: COSMOSIL $_5C_{18}$ AR-II, 4.6 × 250 mm, a linear gradient of 25–45% acetonitrile, 30 min). The eluent was monitored at 220 nm and characterized by ESI-MS. The product was gel filtrated with Sephadex G-10 and purified by RP-HPLC under the same condition as for peptide fragments.

### ESI-MS sample preparation of the folded domain with zinc ion

The synthetic δC1b domain in ultra pure water was treated with 3 molar equivalents of $ZnCl_2$. After incubation at 4 °C for 10 min, the solution was neutralized with 10 mM of pyridinium acetate buffer (pH 6.8). The peptide concentration was adjusted to 50 μM.

### Expression and purification of recombinant δC1b domain

The recombinant δC1b domain was expressed as a GST fusion domain. The protein was purified by GSTrap (GE Healthcare) following the manufacturer instruction, then the GST domain was cleaved by treatment with thrombin at 4 °C for 12 h. The δC1b domain was further purified by size-exclusion chromatography. The purity of the domain was confirmed as >90% by SDS-PAGE [17].

### CD spectroscopy

UV CD spectra were recorded on a Jasco J-720 spectropolarimeter at 25 °C. The measurements were performed using a 0.1 cm path length cuvette at a 0.1 nm spectral resolution. Each spectrum represents the average of ten scans, and the scan rate was 50 nm/min. The initial measurement solution contained 50 μM peptide, 50 mM Tris·HCl (pH 7.5), and 1 mM DTT. $ZnCl_2$ was added to the mixture at 100 μM. To measure the unfolded state of synthetic δC1b domain, EDTA was added to the folded peptide mixture at 100 μM.

### [$^3$H]-phorbol 12, 13-dibutylate binding

[$^3$H]-phorbol 12, 13-dibutyrate (PDBu) binding to PKC was measured by the polyethylene glycol precipitation assay as described in Refs. 15,16 with minor modification. To determine the dissociation constant ($K_d$) for the synthetic δC1b, saturation curves with increasing concentrations of the [$^3$H]PDBu were obtained in triplicate. The 250 μl of assay mixture contained 50 mM Tris·HCl (pH 7.4), 1 mM ethyleneglycol-*bis*(β-aminoethyl)-*N*,*N*,*N*′,*N*′-tetraacetic acid (EGTA), 0.1 mg/ml phosphatidylserine,



*J. Pept. Sci.* 2009; **15**: 642–646  

2 mg/ml bovine immunoglobulin G, variable concentrations of [$^3$H]PDBu and nonspecific line containing the excessive amount of nonradioactive PDBu against [$^3$H]PDBu. After the addition of peptides stored in 0.015% Triton X-100, binding was carried out at 18 °C for 10 min. Samples were incubated on ice for 10 min. To precipitate peptides, 200 µl of 35% polyethylene glycol in 50 mM Tris·HCl (pH 7.4) was added, then vortexed, and the samples were further incubated on ice for 10 min. The tubes were centrifuged at 4 °C (12,200 rpm, 15 min), then 100 µl aliquot of each supernatant was transferred to scintillation vials for the determination of free [$^3$H]PDBu. Remaining supernatant was aspirated off, and the bottom of centrifuge tube was cut off just above the pellet and transferred to a scintillation vial for the determination of total bound [$^3$H]PDBu.

## Results and Discussion

In the synthesis of the δC1b domain, the *N*-terminal (δC1b(231–246)) and *C*-terminal (δC1b(247–281)) peptide fragments were synthesized separately. In this case, an unprotected peptide δC1b(231–246) α-carboxythioester was reacted with another peptide containing an *N*-terminal cysteine residue, δC1b(247–281) [17]. The δC1b(231–246) and δC1b(247–281) fragment peptides were synthesized by Fmoc-based SPPS on a 2-chlorotrityl resin and on a Rink amide resin (NovaSyn TGR), respectively, as described in Materials and Methods Section. The fragment peptides were purified by RP HPLC and characterized by electrospray ionization time-of-flight mass spectrometry (ESI-TOFMS) using a DALTONICS (BRUKER): δC1b(231–246) α-carboxythioester *m/z* [M+H$^+$] calcd: 2203.5, observed: 2203.8; δC1b(247–281) *m/z* [M+H$^+$] calcd: 3829.6, observed: 3829.3. The purification by HPLC (column: COSMOSIL 5C18 AR-II, 20 × 250 mm, a linear gradient of 25–30% acetonitrile in water for δC1b(231–246) α-carboxythioester and a 29% acetonitrile isocratic elution for δC1b(247–281), 30 min) gave pure fragment peptides δC1b(231–246) α-carboxythioester and δC1b(247–281) in overall yields of 35% and 8%, respectively. The purified peptides were lyophilized and dissolved in buffer before the ligation reaction. Charts (A–C) in Figure 1 show the progress of the ligation reaction at 0, 6.5 and 18 h incubation, respectively. The labeled peak c shows thiophenol. The other peaks were identified by ESI-MS; a, δC1b(231–246) (2-mercaptopropionate thioester); b, δC1b(247–281); d, δC1b(231–281) *m/z* [M+H$^+$] calcd: 5898.8, observed: 5899.0. Purification by RP HPLC (column: COSMOSIL 5C18 AR-II, 10 × 250 mm, a linear gradient of 30–45% acetonitrile, 30 min) gave pure δC1b(231–281) in 45% overall yield. Although the δC1b domain contains six cysteine residues, the synthesis of this peptide was efficiently achieved using the ligation technique. Formerly, Futaki *et al.* [18] performed the synthesis of a $Cys_2His_2$-type zinc finger peptide by applying the NCL method. They showed that this method could apply to the synthesis of more than 90 amino acid peptide and that the synthetic peptide shows correct domain folding and zinc ion chelating as a recombinant protein. In their synthesis, the ligation junction was between methionine and cysteine at the linker residues of the zinc finger peptide. For the δC1b domain, we first attempted ligation at Phe243 and Cys244 junction because of slight possibility of epimerization in thioesterification. After confirmation of low reactivity at this junction, His246 and Cys247 junction was adopted as NCL junction. His–Cys junction has been indicated as very fast kinetics (less than 4 h to complete ligation, when compared to Phe–Cys junction which showed approximately 20% reaction after 48 h) residues for NCL reaction. [19]. However, the thioesterification at the *C*-terminal histidine residue could cause epimerization. To avoid epimerization, the reaction was performed under acidic conditions and low temperature (~0 °C) [17]. After NCL reaction, the epimerization of δC1b domain was investigated by isocratic HPLC. To identify the isomer of δC1b domain, D-His incorporated fragment of δC1b(231–246) was synthesized and utilized for NCL. The retention time of D-His δC1b(231–281) was compared with those of L-His domains ligated under −20 and 0 °C. The eluent peaks were identified by ESI-MS. The results indicate that the synthetic δC1b(231–281) contains undetectable level of the isomer form (see Figure S1, Supporting Information).

Folding properties of the peptide were assessed by CD spectra [11]. X-ray crystallography analysis of the δC1b domain has revealed that the domain is a cysteine-rich zinc finger structure with two zinc ions as cofactors [20]. Upon the addition of 2 molar equivalents of zinc ion to the peptide solution, a red-shift at the absorption minimum of the spectrum was observed (Figure 2). The spectrum for the folded δC1b domain was similar to that of the native δC1b domain obtained as a recombinant protein domain. The recombinant δC1b domain was expressed in *Escherichia coli* and purified by GST-affinity chromatography. On the basis of the result that the recombinant domain showed equal ligand binding affinity and folding property as previously described [11], the spectrum was referred as correctly folded state of the domain. To further assess the state of folding of the synthetic δC1b domain, a molar equivalent of EDTA to zinc ion was added. The minimum absorption showed a blue-shift, indicating that the zinc ion plays an important role in the folding of the domain. Furthermore, the molecular weight of the folded domain with zinc ions was characterized by ESI-MS [11]. The charge states of 4+ and 5+ (*m/z*: 1506.6 and 1205.5, respectively) were observed and their reconstructed mass (6023.4) was consistent with the calculated mass of

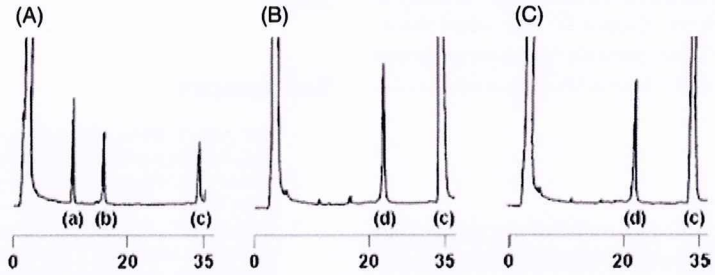


**Figure 1.** HPLC charts of the NCL reaction solution. Charts (A)–(C) show the reaction progress at 0, 6.5, and 18 h incubation, respectively, after the thiophenol addition. Numbers under each chart indicate the elution time (minutes). Peaks (a)–(d) show as follows: a, δC1b(231–246) (2-mercaptopropionate thioester); b, δC1b(247–281); c, thiophenol; d, δC1b(231–281).



  

Journal of PeptideScience

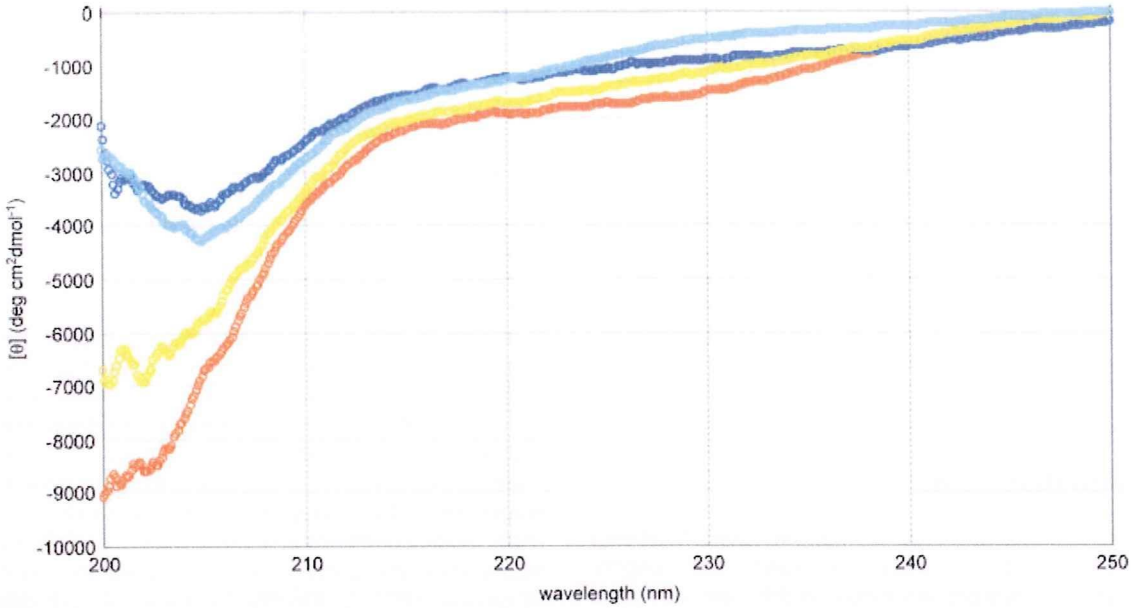


**Figure 2.** CD spectra of the synthetic δC1b peptide in the presence or absence of metals and comparison with that of a recombinant δC1b domain. The buffer contains 50 mM Tris·HCl (pH 7.5) and 1 mM DTT. Spectra shown are as follows: orange dots, peptide (50 μM) only; blue dots, peptide (50 μM) + 100 μM $ZnCl_2$; yellow dots, peptide (50 μM) + 100 μM $ZnCl_2$ + 100 μM EDTA; light blue dots, the recombinant δC1b domain.

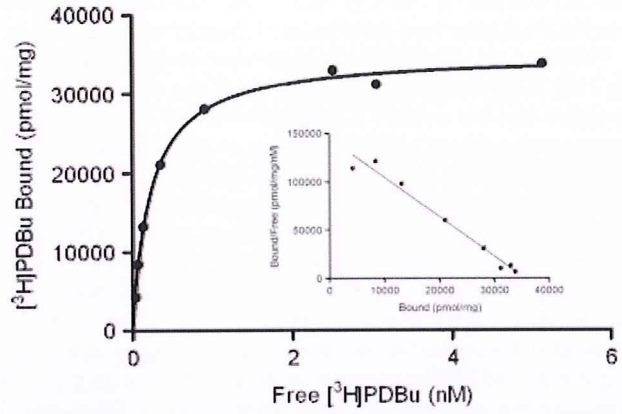


**Figure 3.** Representative saturation curves with increasing concentrations of [$^3$H]PDBu. [$^3$H]PDBu scatchard plots for the synthetic δC1b domain are shown in the panel. Binding was measured using the polyethylene glycol precipitation assay. Each point represents the mean of triplicate determinations, generally with a standard error of 2%. Similar results were obtained in two additional experiments.

δC1b(231–281) + 2Zn − 4H (6022.6) [21]. The ligand binding of the synthetic δC1b domain was assessed by binding assays utilizing [$^3$H]PDBu. The $K_d$ for PDBu was determined to be 0.34 ± 0.08 nM (mean ± SEM, $n$ = 3 experiments) (Figure 3). This value shows that the synthetic δC1b domain is comparable to the recombinant protein domain ($K_d$ = 0.8±0.1 nM) in ligand binding analyses [22].

## Conclusions

In summary, a Cys-rich peptide, PKCδ C1b domain, was successfully synthesized by NCL methodology. In the synthesis of C1b domains by a stepwise condensation method, special reagents and resins such as HATU and PEG-PS resin were utilized on account of difficulty in coupling [11]. The fragment condensation by NCL would be an advantageous alternative method since normal reagents can be used for the synthesis of each fragment. Proper zinc-finger structure folding was determined by CD spectra. The binding of PDBu was assessed by polyethyleneglycol precipitation assays and the result indicated that the synthetic δC1b domain is suitable for use in ligand binding analyses. This methodology makes feasible the efficient preparation of modified C1b domains, which might be useful for the establishment of new binding assay methods or for the characterization of newly synthetic isozyme-specific ligands.

### Acknowledgements

This work was supported in part by a Grant-in-aid from the Ministry of Education, Culture, Sports, Science, and Technology, Japan, and of the Ministry of Health, Labour, and Welfare. It was also supported in part by the Intramural Program of the National Institutes of Health, Center for Cancer Research, National Cancer Institute. The authors thank Professor Kazunari Akiyoshi, Institute of Biomaterials and Bioengineering, Tokyo Medical and Dental University, for his assistance in the CD experiments.

### Supporting information

Supporting information may be found in the online version of this article.

## References

1 Nishizuka Y. Intracellular signaling by hydrolysis of phospholipids and activation of protein kinase C. *Science* 1992; **11**: 607–614.
2 Newton AC. Protein kinase C: structure, function, and regulation. *J. Biol. Chem.* 1995; **270**: 28495–28498.
3 Watanabe T, Ono Y, Taniyama Y, Hazama K, Igarashi K, Ogita K, Kikkawa U, Nishizuka Y. Cell division arrest induced by phorbol ester in CHO cells overexpressing protein kinase C-delta subspecies. *Proc. Natl Acad. Sci. USA* 1992; **89**: 10159–10163.
4 Mischak H, Pierce JH, Goodnight J, Kazanietz G, Blumberg PM, Mushinski JF. Phorbol ester-induced myeloid differentiation is

  

mediated by protein kinase C-alpha and -delta and not by protein kinase C-beta II, -epsilon, -zeta, and -eta. *J. Biol. Chem.* 1993; **268**: 20110–20115.
5 Li C, Wernig E, Leitges M, Hu Y, Xu Q. Mechanical stress-activated PKC$\delta$ regulates smooth muscle cell migration. *FASEB J.* 2003; **17**: 2106–2108.
6 Ghayur T, Hugunin M, Talanian V, Ratnofsky S, Quinlan C, Emoto Y, Pandey P, Datta R, Huang Y, Kharbanda S, Allen H, Kamen R, Wong W, Kufe D. Proteolytic activation of protein kinase C delta by an ICE/CED 3-like protease induces characteristics of apoptosis. *J. Exp. Med.* 1996; **184**: 2399–2404.
7 Humphries MJ, Limesand KH, Schneider JC, Nakayama KI, Anderson SM, Reyland ME. Suppression of apoptosis in the protein kinase C$\delta$ null mouse in vivo. *J. Biol. Chem.* 2006; **281**: 9728–9737.
8 Tamamura H, Sigano DM, Lewin NE, Blumberg PM, Marquez VE. Conformationally constrained analogues of diacylglycerol. 20. The search for an elusive binding site on protein kinase C through relocation of the carbonyl pharmacophore along the sn-1 side chain of 1,2-diacylglycerol lactones. *J. Med. Chem.* 2004; **47**: 644–655.
9 Tamamura H, Sigano DM, Lewin NE, Peach ML, Nicklaus MC, Blumberg PM, Marquez VE. Conformationally constrained analogues of diacylglycerol (DAG). 23. Hydrophobic ligand-protein interactions versus ligand-lipid interactions of DAG-lactones with protein kinase C (PK-C). *J. Med. Chem.* 2004; **47**: 4858–4864.
10 Marquez VE, Blumberg PM. Synthetic diacylglycerols (DAG) and DAG-lactones as activators of protein kinase C (PK-C). *Acc. Chem. Res.* 2003; **36**: 434–443.
11 Irie K, Oie K, Nakahara A, Yanai Y, Ohigashi H, Wender PA, Fukuda H, Konishi H, Kikkawa U. Molecular basis for protein kinase C isozyme-selective binding: the synthesis, folding, and phorbol ester binding of the cysteine-rich domains of all protein kinase C isozymes. *J. Am. Chem. Soc.* 1998; **120**: 9159–9167.
12 Dawson PE, Muir TW, Clark-Lewis I, Kent SBH. Synthesis of proteins by native chemical ligation. *Science* 1994; **266**: 776–779.
13 Dawson PE, Churchill MJ, Ghadiri MR, Kent SBH. Modulation of reactivity in native chemical ligation through the use of thiol additives. *J. Am. Chem. Soc.* 1997; **119**: 4325–4329.
14 von Eggelkraut-Gottanka R, Klose A, Beck-Sickinger AG, Beyermann M. Peptide "thioester formation using standard Fmoc-chemistry. *Tetrahedron Lett.* 2003; **44**: 3551–3554.
15 Sharkey NA, Blumberg PM. Highly lipophilic phorbol esters as inhibitors of specific [3H]phorbol 12,13-dibutyrate binding. *Cancer Res.* 1985; **45**: 19–24.
16 Kazanietz MG, Krausz KW, Blumberg PM. Differential irreversible insertion of protein kinase C into phospholipid vesicles by phorbol esters and related activators. *J. Biol. Chem.* 1992; **267**: 20878–20886.
17 Kajihara Y, Yoshihara A, Hirano K, Yamamoto N. Convenient synthesis of a sialylglycopeptide-thioester having an intact and homogeneous complex-type disialyl-oligosaccharide. *Carbohydr. Res.* 2006; **341**: 1333–1340.
18 Futaki S, Tatsuto K, Shiraishi Y, Sugiura Y. Total synthesis of artificial zinc-finger protein. Problems and perspectives. *Biopolymers* 2004; **76**: 98–109.
19 Hackeng TM, Griffin JH, Dawson PE. Protein synthesis by native chemical ligation: expanded scope by using straightforward methodology. *Proc. Natl Acad. Sci. USA* 1999; **96**: 10068–10073.
20 Zhang G, Kazanietz MG, Blumberg PM, Hurley JH. Crystal structure of the cys2 activator-binding domain of protein kinase C delta in complex with phorbol ester. *Cell* 1995; **81**: 917–924.
21 Tamamura H, Otaka T, Murakami T, Ibuka T, Sakano K, Waki M, Matsumoto A, Yamamoto N, Fujii N. An anti-HIV peptide, T22, forms a highly active complex with Zn(II). *Biochem. Biophys. Res. Commun.* 1996; **229**: 648–652.
22 Kazanietz MG, Wang S, Milne GW, Lewin NE, Liu LH, Blumberg PM. Residues in the second cysteine-rich region of protein kinase C $\delta$ relevant to phorbol ester binding as revealed by site-directed mutagenesis. *J. Biol. Chem.* 1995; **270**: 21852–21859.

  

# Structure-activity relationship study on artificial CXCR4 ligands possessing the cyclic pentapeptide scaffold: the exploration of amino acid residues of pentapeptides by substitutions of several aromatic amino acids†

**Tomohiro Tanaka,[a] Wataru Nomura,*[a] Tetsuo Narumi,[a,b] Ai Esaka,[b] Shinya Oishi,[b] Nami Ohashi,[a] Kyoko Itotani,[a] Barry J. Evans,[c] Zi-xuan Wang,[c,d] Stephen C. Peiper,[c] Nobutaka Fujii[b] and Hirokazu Tamamura*[a]**

*Received 30th April 2009, Accepted 9th June 2009*
*First published as an Advance Article on the web 20th July 2009*
**DOI: 10.1039/b908286g**

Previously, downsizing of a 14-residue peptidic CXCR4 antagonist **1** has led to the development of a highly potent CXCR4 antagonist **2** [*cyclo*(-D-Tyr[1]-Arg[2]-Arg[3]-Nal[4]-Gly[5]-)]. In the present study, cyclic pentapeptide libraries that were designed by substitutions of several amino acids for D-Tyr[1] and Arg[2] in peptide **2** were prepared and screened to evaluate binding activity for CXCR4. The above structure-activity relationship study led to the finding of several potent CXCR4 ligands.

## Introduction

The chemokine receptor CXCR4, which has an endogenous ligand, stromal-cell derived factor-1α (SDF-1α)/CXCL12,[1,2] belongs to the G-protein coupled receptor (GPCR) family.[3,4] The CXCR4-CXCL12 axis plays an important role in various physiological functions: chemotaxis,[5] angiogenesis[6,7] and neurogenesis[8,9] in embryonic stage. However, CXCR4 is also relevant to multiple intractable diseases: AIDS,[10,11] cancer metastasis,[12] progress of leukemia,[13] and rheumatoid arthritis[14] in adulthood. Thus, CXCR4 is thought to be an attractive drug target against these diseases, and CXCR4 antagonists would be useful for the development of potent therapeutic agents.[15–17] Various CXCR4 antagonists such as AMD3100[18,19] and KRH-1636[20] have been reported to date. A 14-residue cyclic peptide CXCR4 antagonist **1** was previously found by structure optimization of an 18-residue bicyclic peptide polyphemusin analogue (Fig. 1).[21,22] Furthermore, the downsizing of **1** using its pharmacophore residues [Arg × 2, L-3-(2-naphthyl)alanine (Nal), Tyr] brought the development of cyclic pentapeptide **2** as a CXCR4 antagonist.[23]

In addition, a biologically stable analogue **3** was derived from **1** with the addition of a 4-fluorobenzoyl group as a new pharmacophore moiety at the N-terminus.[24] We have studied structure-activity-relationship (SAR) of **2** through various modifications such as changes of the ring size and amino acid substitutions.[25–27]

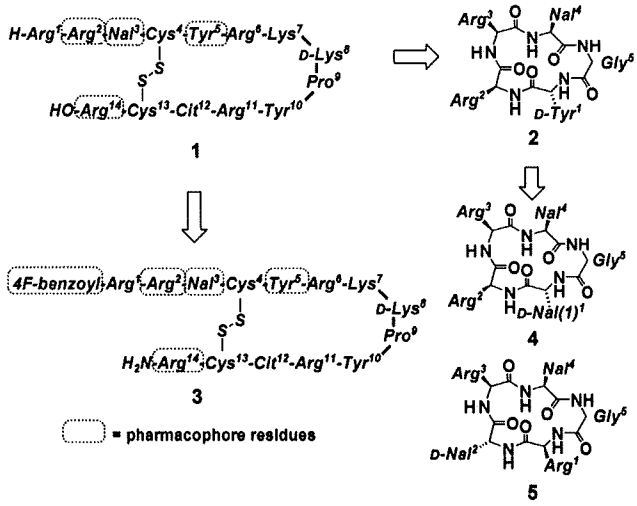


**Fig. 1** Development of a cyclic pentapeptide **2** based on the pharmacophore of a CXCR4 antagonistic peptide **1**. Further conversion from **1** into a biostable derivative **3** and from **2** into new cyclic pentapeptide leads **4** and **5**. Cit = L-citrulline, Nal = L-3-(2-naphthyl)alanine, Nal(1) = L-3-(1-naphthyl)alanine.

Potent CXCR4 ligands contain aromatic and cationic groups,[28] suggesting that these groups are involved in binding to CXCR4 mediated by hydrophobic and electrostatic interactions. In a previous study, D-Tyr[1] and Arg[2] in peptide **2** were replaced by a bicyclic aromatic amino acid and a cationic amino acid to identify novel pharmacophores and to find new lead compounds. Compounds **4**, with replacement of D-Tyr[1] by D-3-(1-naphthyl)alanine (D-Nal(1)), and **5** with the sequence of Arg[1]-D-Nal[2] based on shuffling cationic and aromatic amino acids at positions 1 and 2 of compound **2** showed high CXCR4 binding activity.[29] Thus, in this study, the design of a cyclic pentapeptide library based on substitutions of several aromatic amino acids at positions 1 and 2 led to the development of novel analogues of **2** to explore new pharmacophore moieties.

[a]*Institute of Biomaterials and Bioengineering, Tokyo Medical and Dental University, Chiyoda-ku, Tokyo, 101-0062, Japan. E-mail: nomura.mr@tmd.ac.jp, tamamura.mr@tmd.ac.jp; Fax: +813 5280 8039; Tel: +813 5280 8036*
[b]*Graduate School of Pharmaceutical Sciences, Kyoto University, Sakyo-ku, Kyoto, 606-8501, Japan*
[c]*Department of Pathology, Anatomy and Cell Biology, Thomas Jefferson University, Philadelphia, PA 19107, USA*
[d]*Department of Surgery, Thomas Jefferson University, Philadelphia, PA 19107, USA*

† Electronic supplementary information (ESI) available: Characterization data (MS and $[\alpha]_D$) and HPLC charts of novel synthetic compounds. See DOI: 10.1039/b908286g

**Table 1** Inhibitory activity of the synthetic compounds **6–10** against binding of [$^{125}$I]-SDF-1α to CXCR4

| Compd | *cyclo*(-**Xaa$^1$**-**Xaa$^2$**-Arg$^3$-Nal$^4$-Gly$^5$-). **Xaa$^1$-Xaa$^2$** | $IC_{50}$/μM[a] |
|---|---|---|
| **2** | D-Tyr$^1$-Arg$^2$ | 0.0079 |
| **6** | D-Phe(4-F)$^1$-Arg$^2$ | 0.22 |
| **7** | D-Phe(4-F)$^1$-D-Arg$^2$ | 0.31 |
| **8** | Phe(4-F)$^1$-Arg$^2$ | 0.22 |
| **9** | Phe(4-F)$^1$-D-Arg$^2$ | 2.2 |
| **10** | *cyclo*(-D-Tyr$^1$-Arg$^2$-Arg$^3$-Nal$^4$- Phe(4-F)$^5$-) | 4.4 |

[a] $IC_{50}$ values are the concentrations for 50% inhibition of the [$^{125}$I]-SDF-1α binding to CXCR4 transfectants of CHO cells. All data are the mean values for at least three experiments.

## Biological results and discussion

### SAR of analogues with L/D-Phe(4-F)$^1$-L/D-Arg$^2$

Since compound **6**, where D-Tyr$^1$ of **2** was replaced by 4-fluoro-D-phenylalanine [D-Phe(4-F)] relevant to the new pharmacophore 4-fluorobenzoyl group, showed relatively potent CXCR4-binding activity as reported previously,[26] initially, **6** and its three analogues **7–9**, [L/D-Phe(4-F)$^1$, L/D-Arg$^2$]-**2**, were synthesized to evaluate the configuration effects of amino acids at positions 1 and 2 (Table 1). These analogues except for **9** showed high CXCR4 binding activity ($IC_{50}$ = 0.2–0.4 μM, Table 1), although the potencies were much lower than that of **2**. Compound **9** showed moderate potency ($IC_{50}$ = 2.2 μM), suggesting that the combination of Phe(4-F)$^1$ and D-Arg$^2$ is not suitable. In addition, compound **10** was synthesized, where Gly$^5$ of **2** was replaced by Phe(4-F) with maintenance of D-Tyr$^1$, since both Phe(4-F) and D-Tyr are thought to be important pharmacophore residues. However, compound **10** did not show high potency ($IC_{50}$ = 4.4 μM), probably due to a conformational change.

### SAR of analogues with replacement of D-Phe(4-F)$^1$ of 6 by an aromatic D-amino acid

Based on the configuration of [D-Phe(4-F)$^1$, L-Arg$^2$] of **6**, a series of analogues with replacement of D-Phe(4-F)$^1$ by several aromatic amino acids were synthesized. The order of preference of halogen atoms as a substituent of position 4 on D-Phe$^1$ is fluorine, chlorine and bromine as shown in activity of **6**, **11** and **12** ($IC_{50}$ = 0.22, 1.2 and 2.3 μM, respectively, Tables 1 & 2). It suggests that a small or electron-withdrawing group is favorable for a substituent of position 4 on D-Phe$^1$. Next, preference of positions of fluorine on the phenyl ring of D-Phe$^1$ was investigated. As a result, the order of preference is *ortho*, *meta* and *para*-positions, as shown in activity of **13**, **14** and **6** ($IC_{50}$ = 0.059, 0.088 and 0.22 μM, respectively). In the previous paper, a D-Nal(1)$^1$-substituted analogue **4** ($IC_{50}$ = 0.043 μM) showed much higher CXCR4 binding activity than a D-Nal$^1$-substituted analogue, [D-Nal$^1$]-**2** ($IC_{50}$ > 2.0 μM).[29] Taken together, a *para*-substituent on the phenyl ring of the D-amino acid residue at position 1 is not appropriate for high potency, possibly due to the steric hindrance between the para-substituent on the phenyl ring and CXCR4. In addition, two other analogues were prepared. Compound **15**, [L/D-Phg$^1$]-**2** (racemic), did not show high CXCR4 binding activity. Compound **16**, [β-(2-thienyl)-D-alanine (D-Thi)$^1$]-**2**, showed very potent CXCR4 binding activity, suggesting a thienyl group is relatively suitable for the side-chain of the amino acid at position 1. New leads, **13** and **16**, having D-Phe(2-F)$^1$ and D-Thi$^1$, respectively, were found although the potencies were approximately one-eighth of that of **2**.

**Table 2** Inhibitory activity of the synthetic compounds **11–16** against binding of [$^{125}$I]-SDF-1α to CXCR4

| Compd | *cyclo*(-**Xaa$^1$**-Arg$^2$-Arg$^3$-Nal$^4$-Gly$^5$-). **Xaa$^1$** | $IC_{50}$/μM[a] |
|---|---|---|
| **2** | D-Tyr$^1$ | 0.0079 |
| **11** | D-Phe(4-Cl)$^1$ | 1.2 |
| **12** | D-Phe(4-Br)$^1$ | 2.3 |
| **13** | D-Phe(2-F)$^1$ | 0.059 |
| **14** | D-Phe(3-F)$^1$ | 0.088 |
| **15** | L/D-Phg$^1$ | 1.1 |
| **16** | D-Thi$^1$ | 0.056 |

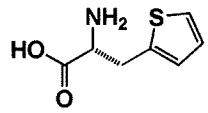


β-(2-thienyl)-D-alanine (D-Thi)

[a] $IC_{50}$ values are the concentrations for 50% inhibition of the [$^{125}$I]-SDF-1α binding to CXCR4 transfectants of CHO cells. All data are the mean values for at least three experiments.

### SAR of analogues with Arg$^1$-aromatic D-amino acid$^2$

Since **5**, an analogue with the sequence of Arg$^1$-D-Nal$^2$ based on shuffling cationic and aromatic amino acids at positions 1 and 2 of compound **2**, showed high CXCR4 binding activity,[29] a series of analogues with the sequence of Arg$^1$-aromatic D-amino acid$^2$ (substitution for D-Nal$^2$) were synthesized. Among halogen substituents at position 4 on the phenyl ring of D-Phe$^2$, fluorine is the most suitable, whereas chlorine or bromine is not preferable as shown in activity of **17**,[26] **18** and **19** ($IC_{50}$ = 0.035, 0.79 and 0.57 μM, respectively, Table 3). In addition, a 4-nitro group is not suitable although this group is an electron-withdrawing group, possibly due to steric hindrance (**20**, $IC_{50}$ = 0.94 μM). A 4-hydroxy group with electron-donating action and a 4-amino group with strong electron-donating action is not favorable (**21**, $IC_{50}$ = 0.97 μM, **22**, $IC_{50}$ = 15 μM). As a result, fluorine is the most suitable substituent at position 4 on D-Phe$^2$ among these atoms and groups. In the investigation of the preference of positions of fluorine on the phenyl ring of D-Phe$^2$, *para*-position is superior to

**Table 3** Inhibitory activity of the synthetic compounds **17–24** against binding of [$^{125}$I]-SDF-1α to CXCR4

| Compd | *cyclo*(-**Xaa$^1$**- **Xaa$^2$**-Arg$^3$-Nal$^4$-Gly$^5$-). **Xaa$^1$-Xaa$^2$** | $IC_{50}$/μM[a] |
|---|---|---|
| **2** | D-Tyr$^1$-Arg$^2$ | 0.0079 |
| **17** | Arg$^1$-D-Phe(4-F)$^2$ | 0.035 |
| **18** | Arg$^1$-D-Phe(4-Cl)$^2$ | 0.79 |
| **19** | Arg$^1$-D-Phe(4-Br)$^2$ | 0.57 |
| **20** | Arg$^1$-D-Phe(4-$NO_2$)$^2$ | 0.94 |
| **21** | Arg$^1$-D-Tyr$^2$ | 0.97 |
| **22** | Arg$^1$-D-Phe(4-$NH_2$)$^2$ | 15 |
| **23** | Arg$^1$-D-Phe(2-F)$^2$ | 7.1 |
| **24** | Arg$^1$-D-Phe(3-F)$^2$ | 6.1 |

[a] $IC_{50}$ values are the concentrations for 50% inhibition of the [$^{125}$I]-SDF-1α binding to CXCR4 transfectants of CHO cells. All data are the mean values for at least three experiments.

**Table 4** Inhibitory activity of the synthetic compounds **25–31** against binding of [$^{125}$I]-SDF-1α to CXCR4

| Compd | *cyclo*(-D-Tyr$^1$-**Xaa$^2$-Xaa$^3$**-Nal$^4$-Gly$^5$-). **Xaa$^2$-Xaa$^3$** | $IC_{50}$/μM[a] |
|---|---|---|
| **2** | Arg$^2$-Arg$^3$ | 0.0079 |
| **25** | Hph$^2$-Arg$^3$ | 0.075 |
| **26** | D-Phg$^2$-Arg$^3$ | 6.0 |
| **27** | Phg$^2$-Arg$^3$ | 0.17 |
| **28** | His$^2$-Arg$^3$ | 0.037 |
| **29** | D-His$^2$-Arg$^3$ | 0.035 |
| **30** | Arg$^2$-His$^3$ | 5.0 |
| **31** | His$^2$-His$^2$ | 12 |

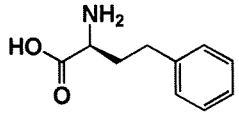

L-homophenylalanine (Hph)

[a] $IC_{50}$ values are the concentrations for 50% inhibition of the [$^{125}$I]-SDF-1α binding to CXCR4 transfectants of CHO cells. All data are the mean values for at least three experiments.

**Table 5** Inhibitory activity of the synthetic compounds **32–37** against binding of [$^{125}$I]-SDF-1α to CXCR4

| Compd | *cyclo*(-**Xaa$^1$**- **Xaa$^2$**-Arg$^3$-Nal$^4$-Gly$^5$-). **Xaa$^1$-Xaa$^2$** | $IC_{50}$/μM[a] |
|---|---|---|
| **2** | D-Tyr$^1$-Arg$^2$ | 0.0079 |
| **32** | Arg$^1$-His$^2$ | 0.40 |
| **33** | Arg$^1$-D-His$^2$ | 0.96 |
| **34** | Arg$^1$-D-Thi$^2$ | 1.7 |
| **35** | Arg$^1$-D-Tpi$^2$ | 8.1 |
| **36** | Arg$^1$-D-Hph$^2$ | 5.0 |
| **37** | Arg$^1$-L/D-Phg$^2$ | 5.9 |

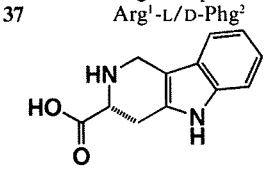

(3*R*)-2,3,4,9-tetrahydro-1*H*-β-carboline -3-carboxylic acid (D-Tpi)

[a] $IC_{50}$ values are the concentrations for 50% inhibition of the [$^{125}$I]-SDF-1α binding to CXCR4 transfectants of CHO cells. All data are the mean values for at least three experiments.

*ortho* or *meta* as shown in the activity of **17**, **23** and **24** ($IC_{50}$ = 0.035, 7.1 and 6.1 μM, respectively). In the previous paper, a D-Nal$^2$-substituted analogue **5** ($IC_{50}$ = 0.045 μM) showed much higher CXCR4 binding activity than a D-Nal(1)$^2$-substituted analogue, [Arg$^1$-D-Nal(1)$^2$]-**2** ($IC_{50}$ > 2.0 μM).[29] Taken together, a *para*-substituent on the phenyl ring of the D-amino acid residue at position 2 is suitable for high potency, possibly due to hydrophobic or π interaction between the *para*-substituent on the phenyl ring and the receptor CXCR4.

### SAR of analogues with replacement of Arg$^2$ of 2 by an aromatic amino acid

Since [D-Tyr$^1$-Phe(4-F)$^2$]-**2** showed high CXCR4 binding activity in the previous paper,[26] analogues having incorporation of an aromatic amino acid into position 2 were synthesized. An L-homophenylalanine (Hph)-substituted analogue **25** showed potent CXCR4 binding activity ($IC_{50}$ = 0.075 μM, Table 4), whereas an L-phenylglycine (Phg)-substituted analogue **27** showed lower CXCR4 binding activity ($IC_{50}$ = 0.17 μM), although a D-phenylglycine (D-Phg)-substituted analogue **26** showed even lower CXCR4 binding activity ($IC_{50}$ = 6.0 μM). Since His has both basic and aromatic character, it would be a useful amino acid substitution at position 2. Practically, L- and D-His-substituted analogues **28** and **29** showed high potency ($IC_{50}$ = 0.037 and 0.035 μM, respectively), indicating that the chirality of L/D-His at position 2 does not affect CXCR4 binding. The potencies are approximately one-fourth of that of **2**. Next, we extended the His-substitution to position 3 (Arg$^3$). Analogues with the sequences of Arg$^2$-His$^3$ and His$^2$-His$^3$ were synthesized (**30** and **31**, respectively). However, these analogues did not show potent CXCR4 binding activity ($IC_{50}$ = 5.2 and 12 μM, respectively), suggesting that His-substitution for Arg$^3$ is not appropriate.

### SAR of analogues with Arg$^1$-aromatic-amino acid$^2$

Among analogues with a combination of the sequences of Arg/His$^2$-Arg/His$^3$, **28** having the sequence of His$^2$-Arg$^3$ is the most potent compound, with almost the same CXCR4 binding activity as **29** (D-His$^2$-Arg$^3$). Thus, **32** and **33**, where D-Tyr$^1$ of **28** and **29** was replaced by Arg, respectively, were synthesized. However, **32** and **33** are more than 10 fold weaker than **28** and **29** (Table 5), indicating that Arg$^1$ is not suitable in these analogues. D-Thi, (3*R*)-2,3,4,9-tetrahydro-1*H*-β-carboline-3-carboxylic acid (D-Tpi), D-Hph and L/D-Phg (racemic)-substituted analogues did not show high potency as shown in **34**, **35**, **36** and **37**, respectively. It suggests that these series of analogues with the sequence of Arg$^1$-aromatic-amino acid$^2$ are not potent compounds, although **5** and **17** showed high potency.

### SAR of analogues with D-Phe(4-F)$^1$-Arg/His$^2$-Arg/His$^3$ or Arg/His$^1$-D-Phe(4-F)$^2$-Arg/His$^3$

Since **6**, [D-Phe(4-F)$^1$]-**2**, showed moderate CXCR4 binding activity,[26] a series of analogues with the sequence of D-Phe(4-F)$^1$-Arg/His$^2$-Arg/His$^3$ were synthesized (**38**, **39** and **40**). However, significantly potent analogues could not be found ($IC_{50}$ > 10 μM, Table 6). Thus, to interchange the order of positions 1 and 2, a series of analogues with the sequence of Arg/His$^1$-D-Phe(4-F)$^2$-Arg/His$^3$ were synthesized (**41**, **42** and **43**). CXCR4 binding

**Table 6** Inhibitory activity of the synthetic compounds **38–43** against binding of [$^{125}$I]-SDF-1α to CXCR4

| Compd | *cyclo*(-**Xaa$^1$**- **Xaa$^2$-Xaa$^3$**-Nal$^4$-Gly$^5$-). **Xaa$^1$-Xaa$^2$-Xaa$^3$** | $IC_{50}$/μM[a] |
|---|---|---|
| **2** | D-Tyr$^1$-Arg$^2$-Arg$^3$ | 0.0079 |
| **38** | D-Phe(4-F)$^1$-Arg$^2$-His$^3$ | 22 |
| **39** | D-Phe(4-F)$^1$-His$^2$-Arg$^3$ | 10 |
| **40** | D-Phe(4-F)$^1$-His$^2$-His$^3$ | >100 |
| **41** | Arg$^1$-D-Phe(4-F)$^2$-His$^3$ | >100 |
| **42** | His$^1$-D-Phe(4-F)$^2$-Arg$^3$ | 5.7 |
| **43** | His$^1$-D-Phe(4-F)$^2$-His$^3$ | >100 |

[a] $IC_{50}$ values are the concentrations for 50% inhibition of the [$^{125}$I]-SDF-1 binding to CXCR4 transfectants of CHO cells. All data are the mean values for at least three experiments.

activities of these analogues are relatively weak ($IC_{50}$ > 5 μM), indicating that incorporation of D-Phe(4-F) at position 1 and His-substitution for $Arg^3$ are not suitable.

## Conclusion

In this paper, SAR of several cyclic pentapeptides having CXCR4 binding activity was studied to discover useful lead compounds. (1) Of the analogues with replacement of D-$Tyr^1$ of **2** by an aromatic D-amino acid, a D-$Phe(2\text{-}F)^1$-substituted analogue, **13**, and a D-$Thi^1$-substituted analogue, **16**, have potent CXCR4 binding activity. A para-substituent on the phenyl ring of the D-amino acid residue at position 1 is not favorable for high potency. (2) Among a series of analogues based on shuffling cationic and aromatic amino acids at positions 1 and 2, an [$Arg^1$-D-$Phe(4\text{-}F)^2$]-containing analogue, **17**, showed the most potent CXCR4 binding activity. A *para*-substituent on the phenyl ring of the D-amino acid residue at position 2 is suitable for high potency. (3) Analogues, where $Arg^2$ of **2** was replaced by L/D-His which have both basic and aromatic characters, have high CXCR4 binding activity. (4) $Arg^1$-substituted analogues or $His^3$-substituted analogues are not potent leads. Taken together, in the present study several new leads were found, and aromatic amino acid residues, Phe(2-F), Phe(4-F), Thi and His, were identified to be new pharmacophore residues in addition to Arg, Nal, Nal(1) and Tyr. The present data will be important for the development of CXCR4 antagonists. In future, the introduction of fluorophenyl, thienyl, imidazoyl groups, *etc.* involving the combinational use of the above groups into the cyclic pentapeptide templates and into low molecular weight linear type scaffolds will bring us the development of new-type leads of CXCR4 antagonists. The present data of preferences of the target CXCR4 such as inclination of aromatic and basic groups will be useful to disclose an unknown detail binding mode of CXCR4 and cyclic pentapeptide-type ligands on the cell membrane.

## Experimental

### Chemistry

Cyclic peptides were synthesized by Fmoc-based solid-phase synthesis followed by cleavage from the resin, cyclization with the diphenylphosphoryl azide and deprotection, as reported previously.[23]

**General.** The protected peptide resin (0.100 mmol), which was constructed on H-Gly-(2-chloro)trityl resin manually by Fmoc-based solid phase peptide synthesis (SPPS). *t*-Bu for L/D-Tyr and Pbf for L/D-Arg were used for side-chain protection. Fmoc deprotection was achieved by 20% (v/v) piperidine in DMF (10 mL, 2 × 1 min, 1 × 20 min). Fmoc amino acids were coupled by treatment with five equivalents of reagents [Fmoc-amino acid, *N*,*N*′-diisopropylcarbodiimide (DIPCDI) and HOBt·$H_2O$] to free amino group in DMF (5 mL) for 1.5 h. The constructed protected peptide resin was subjected to AcOH/TFE/$CH_2Cl_2$ (1 : 1 : 3 (v/v/v), 10 mL) treatment at room temperature for 2 h. After filtration of the residual resin, the filtrate was concentrated under reduced pressure to give a crude protected peptide. To a stirred mixture of the protected peptide and $NaHCO_3$ (57.1 mg, 0.680 mmol) in DMF (41 mL) was added diphenylphosphoryl azide (DPPA, 0.0879 mL, 0.408 mmol) at −40 °C. The mixture was stirred for 36 h with warming to room temperature and filtered. The filtrate was concentrated under reduced pressure to give an oily residue, which was subjected to solid phase extraction over basic alumina in $CHCl_3$-MeOH (9 : 1 (v/v)) to remove inorganic salts derived from DPPA. The resulting cyclic protected peptide was treated with 95% TFA solution for 1.5 h at room temperature. Concentration under reduced pressure and purification by preparative HPLC gave a cyclic peptide.

### CXCR4 receptor binding assay[30]

Stable CHO cell transfectants expressing CXCR4 were prepared as described previously.[31] CHO transfectants were detached by treatment with trypsin-EDTA, allowed to recover in complete growth medium (MEM-R, 100 μg/mL penicillin, 100 μg/mL streptomycin, 0.25 μg/mL amphotericin B, 10% FBS (v/v)), and then washed in cold binding buffer (PBS containing 2 mg/mL BSA). For ligand binding, the cells were resuspended in binding buffer at $1 \times 10^7$ cell/mL, and 100 μL aliquots were incubated with 0.1 nM of [$^{125}$I]-SDF-1 (Perkin-Elmer Life Sciences) for 1 h on ice under constant agitation. Free and bound radioligands were separated by centrifugation of the cells through an oil cushion, and bound radioactivity was measured with a gamma-counter (Cobra, Packard, Downers Grove, IL, USA). Inhibitory activity of test compounds was determined based on the inhibition of [$^{125}$I]-SDF-1 binding to CXCR4 transfectants ($IC_{50}$).


## Acknowledgements

This work was supported by New Energy and Industrial Technology Development Organization (NEDO), Grant-in-Aid for Scientific Research from the Ministry of Education, Culture, Sports, Science, and Technology of Japan, and Health and Labour Sciences Research Grants from Japanese Ministry of Health, Labor, and Welfare.


## References


1 K. Tashiro, H. Tada, R. Heilker, M. Shirozu, T. Nakano and T. Honjo, *Science*, 1993, **261**, 600–603.
2 T. Nagasawa, H. Kikutani and T. Kishimoto, *Proc. Natl. Acad. Sci. U. S. A.*, 1994, **91**, 2305–2309.
3 M. Loetscher, T. Geiser, T. O'Reilly, R. Zwahlen, M. Baggiolini and B. Moser, *J. Biol. Chem.*, 1994, **269**, 232–237.
4 B. J. Rollins, *Blood*, 1997, **90**, 909–928.
5 C. C. Bleul, R. C. Fuhlbrigge, J. M. Casanovas, A. Aiuti and T. A. Springer, *J. Exp. Med.*, 1996, **2**, 1101–1109.
6 K. Tachibana, S. Hirota, H. Iizasa, H. Yoshida, K. Kawabata, Y. Kataoka, Y. Kitamura, K. Matsushima, N. Yoshida, S. Nishikawa, T. Kishimoto and T. Nagasawa, *Nature*, 1998, **393**, 591–594.
7 T. Nagasawa, S. Hirota, K. Tachibana, N. Takakura, S. Nishikawa, Y. Kitamura, N. Yoshida, H. Kikutani and T. Kishimoto, *Nature*, 1996, **382**, 635–638.
8 Y. Zhu, Y. Yu, X. C. Zhang, T. Nagasawa, J. Y. Wu and Y. Rao, *Nat. Neurosci.*, 2002, **5**, 719–720.
9 R. K. Stumm, C. Zhou, T. Ara, F. Lazarini, M. Dubois-Dalcq, T. Nagasawa, V. Hollt and S. Schulz, *J. Neurosci.*, 2003, **23**, 5123–5130.

10 E. Oberlin, A. Amara, F. Bachelerie, C. Bessia, J. L. Virelizier, F. Arenzana-Seisdedos, O. Schwartz, J. M. Heard, I. Clark-Lewis, D. L. Legler, M. Loetscher, M. Baggiolini and B. Moser, *Nature*, 1996, **382**, 833–835.
11 Y. Feng, C. C. Broder, P. E. Kennedy and E. A. Berger, *Science*, 1996, **272**, 872–877.
12 A. Müller, B. Homey, H. Soto, N. Ge, D. Catron, M. E. Buchanan, T. Mcclanahan, E. Murphy, W. Yuan, S. M. Wagner, J. L. Barrera, A. Mohar, E. Vera'stegui and A. Zlotnik, *Nature*, 2001, **410**, 50–56.
13 J. A. Burger, M. Burger and T. J. Kipps, *Blood*, 1999, **94**, 3658–3667.
14 T. Nanki, K. Hayashida, H. S. EI-Gabalawy, S. Suson, K. Shi, H. J. Girschick, S. Yavuz and P. E. Lipsky, *J. Immunol.*, 2000, **165**, 6590–6598.
15 T. Murakami, T. Nakajima, Y. Koyanagi, K. Tachibana, N Fujii, H. Tamamura, N. Toshida, M. Waki, A. Matsumoto, O. Yoshie, T. Kishimoto, N. Yamamoto and T. Nagasawa, *J. Exp. Med.*, 1997, **186**, 1389–1393.
16 H. Tamamura, A. Hori, N. Kanzaki, K. Hiramatsu, M. Mizumoto, H. Nakashima, N. Yamamoto, A. Otaka and N. Fujii, *FEBS Lett.*, 2003, **550**, 79–83.
17 H. Tamamura, M. Fujisawa, K. Hiramatsu, M. Mizumoto, H. Nakashima, N. Yamamoto, A. Otaka and N Fujii, *FEBS Lett.*, 2004, **569**, 99–104.
18 D. Schols, S. Struyf, J. Van Damme, J. A. Este, G. Henson and E. DeClarcq, *J. Exp. Med.*, 1997, **186**, 1383–1388.
19 G. A. Donzella, D. Schols, S. W. Lin, J. A. Este and K. A. Nagashima, *Nat. Med.*, 1998, **4**, 72–76.
20 K. Ichiya, S. Yokoyama-Kumakura, Y. Tanaka, R. Tanaka, K. Hirose, K. Bannai, T. Edamatsu, M. Yanaka, Y. Niitani, N. Miyano-Kurosaki, H. Takaku, Y. Koyanagi and N. Yamamoto, *Proc. Natl. Acad. Sci. U. S. A.*, 2003, **100**, 4185–4190.
21 M. Masuda, H. Nakashima, T. Ueda, H. Naba, R. Ikoma, A. Otaka, Y. Terakawa, H. Tamamura, T. Ibuka, T. Murakami, Y. Koyanagi, M. Waki, A. Matsumoto, N. Yamamoto and N. Fujii, *Biochem. Biophys. Res. Commun.*, 1992, **189**, 845–850.
22 Tamamura, Y Xu, T. Hattori, X. Zhang, R. Arakaki, K. Kanbara, A. Omagari, A. Otaka, T. Ibuka, N. Yamamoto, H. Nakashima and N. Fujii, *Biochem. Biophys. Res. Commun.*, 1998, **253**, 877–882.
23 N. Fujii, S. Oishi, K. Hiramatsu, T. Araki, S. Ueda, H. Tamamura, A. Otaka, S. Kusano, S. Terakubo, H. Nakashima, J. A. Broach, J. O. Trent, Z. Wang and S. C. Peiper, *Angew. Chem., Int. Ed.*, 2003, **42**, 3251–3253.
24 H. Tamamura, K. Hiramatsu, M. Mizumoto, S. Ueda, S. Kusano, S. Terakubo, M. Akamatsu, N. Yamamoto, J. O. Trent, Z. Wang, S. C. Peiper, H. Nakashima, A. Otaka and N. Fujii, *Org. Biomol. Chem.*, 2003, **1**, 3663–3669.
25 H. Tamamura, T. Araki, S. Ueda, Z. Wang, S. Oishi, A. Esaka, J. O. Trent, H. Nakashima, N. Yamamoto, S. C. Peiper, A. Otaka and N. Fujii, *J. Med. Chem.*, 2005, **48**, 3280–3289.
26 H. Tamamura, A. Esaka, T. Ogawa, T. Araki, S. Ueda, Z. Wang, J. O. Trent, H. Tsutsumi, H. Masuno, H. Nakashima, N. Yamamoto, S. C. Peiper, A. Otaka and N. Fujii, *Org. Biomol. Chem.*, 2005, **3**, 4392–4394.
27 S. Ueda, S. Oishi, Z. Wang, T. Araki, H. Tamamura, J. Cluzeau, H. Ohno, S. Kusano, H. Nakashima, J. O. Trent, S. C. Peiper and N. Fujii, *J. Med. Chem.*, 2007, **50**, 192–198.
28 W. Zhan, Z. Liang, A. Zhu, S. Kurtkaya, H. Shim, J. P. Snyder and D. C. Liotta, *J. Med. Chem.*, 2007, **50**, 5655–5664.
29 T. Tanaka, H. Tsutsumi, W. Nomura, Y. Tanabe, N. Ohashi, A. Esaka, C. Ochiai, J. Sato, K. Itotani, T. Murakami, K. Ohba, N. Yamamoto, N. Fujii and H. Tamamura, *Org. Biomol. Chem.*, 2008, **6**, 4374–4377.
30 H. Tamamura, K. Hiramatsu, S. Kusano, S. Terakubo, N. Yamamoto, J. O. Trent, Z. Wang, S. C. Peiper, H. Nakashima, A. Otaka and N. Fujii, *Org. Biomol. Chem.*, 2003, **1**, 3656–3662.
31 J. M. Navenot, Z. X. Wang, J. O. Trent, J. L. Murray, Q. X. Hu, L. DeLeeuw, P. S. Moore, Y. Chang and S. C. Peiper, *J. Mol. Biol.*, 2001, **59**, 380–393.

Protein Imaging

DOI: 10.1002/anie.200903183

# Fluorogenically Active Leucine Zipper Peptides as Tag–Probe Pairs for Protein Imaging in Living Cells**

*Hiroshi Tsutsumi, Wataru Nomura, Seiichiro Abe, Tomoaki Mino, Akemi Masuda, Nami Ohashi, Tomohiro Tanaka, Kenji Ohba, Naoki Yamamoto, Kazunari Akiyoshi, and Hirokazu Tamamura**

Artificial functional peptides are valuable tools in various fields of chemical biology. Small peptides, such as an oligohistidine tag (His tag), can be genetically incorporated into target proteins and used for purification of recombinant proteins, immobilization of proteins on microplates, and bioimaging of proteins on the surface of living cells with their complementary partner molecules, such as $Ni^{II}$–nitrilotriacetic acid complex ($Ni^{II}$-NTA).[1] Tsien and co-workers reported that pairs of tetracysteine motif peptides and biarsenical molecular probes, which specifically bind to tetracysteine peptides, are useful in the real-time fluorescence imaging of proteins in living cells.[2] Several pairs of other tag peptides/proteins and their specific ligands have also been reported.[3,4] In many cases, however, the bound/free (B/F) separation process of probes is necessary to avoid background emission from excess probe molecules. Fluorogenic tag–probe pairs can facilitate in distinguishing the labeled proteins from the free probes, without the B/F separation process. However, very few tag–probe pairs have been developed to date.[2a]

Engineered leucine zipper peptides, which have complementary selectivity and strong binding affinity, have been applied to tags for the affinity purification of expressed proteins, to anchors for immobilization of proteins on microplates, and to allosteric modulators of engineered enzyme activity.[5] Moreover, the hydrophobic cores of leucine zipper peptides can be engineered to form hydrophobic pockets in which small organic molecules can bind.[6] It is thought that selective binding of environmentally sensitive fluorescent dyes to these pockets inside the leucine zipper assembly might induce colorimetric changes and enhance their fluorescence intensity. The unique characteristics of leucine zipper peptides might enable production of fluorescent tag–probe pairs that are exchangeable. Herein, we describe the development of a fluorescent changeable tag–probe system based on artificial leucine zipper peptides, designated ZIP tag–probe pairs, and its application to the fluorescence imaging of ZIP tag–fused protein on the surface of living cells.

The design of ZIP tag–probe pairs is based on the crystal structure of an antiparallel coiled-coil trimer of a GCN4 mutant (Figure 1).[7] The probe peptide is an α-helical peptide with 4-nitrobenzo-2-oxa-1,3-diazole (NBD), an environmentally sensitive fluorescent dye, attached to the side chain of L-α-2,3-diaminopropionic acid, that is, Dap(NBD). Tag peptides are designed as antiparallel 2α-helical peptides linked through a Gly–Gly–Cys–Gly–Gly loop sequence. Two leucine residues, which are located at the positions complementary to the NBD in the probe peptide, are replaced by alanine or glycine so that hydrophobic pockets will be formed when the tag peptides bind to the probe peptide. Original tag peptides having two leucine residues at the complementary positions are designated as L2, and alanine- or glycine-substituted tag peptides are designated as A2 and G2, respectively.

In the UV/Vis analysis, the absorption spectra of the probe peptide changed on addition of A2 producing isosbestic points at 456, 403, and 333 nm, and thus the excitation wavelength was determined as 456 nm (Figure S1 in the Supporting Information). A fluorescence titration experiment revealed that the fluorescence spectra of the probe peptide changed remarkably with increasing A2 concentration. The emission maximum arising from the NBD dye showed a significant blue shift from 536 to 505 nm with a concurrent increase in the emission intensity (Figure 2a,b and Table 1). Such a spectral change clearly suggests that the NBD moiety of the probe peptide is located in the hydrophobic environment within the 3α-helical peptide bundle structure, which is supported by the previous report of Uchiyama et al.[8]

In the cases of L2 and G2, similar spectral changes were observed although the wavelength shifts and changes in fluorescence intensity were less than those in the case of A2 (Figure S2 in the Supporting Information and Table 1). As there is insufficient space to accommodate an NBD moiety in the complex of the L2–probe pair, the NBD moiety might bind only to the hydrophobic surface of two leucine residues of L2, thus causing the subtle fluorescence change. The

[*] S. Abe, T. Mino, A. Masuda, Prof. K. Akiyoshi, Prof. H. Tamamura
Institute of Biomaterials and Bioengineering
Tokyo Medical and Dental University
Chiyoda-ku, Tokyo 101-0062 (Japan)
and
School of Biomedical Science, Tokyo Medical and Dental University
Chiyoda-ku, Tokyo 101-0062 (Japan)
Fax: (+81) 3-5280-8036
E-mail: tamamura.mr@tmd.ac.jp
Dr. H. Tsutsumi, Dr. W. Nomura, N. Ohashi, T. Tanaka
Institute of Biomaterials and Bioengineering
Tokyo Medical and Dental University
Chiyoda-ku, Tokyo 101-0062 (Japan)
Dr. K. Ohba, Prof. N. Yamamoto
AIDS Research Center, National Institute of Infectious Diseases
Shinjuku-ku, Tokyo 162-8640 (Japan)

[**] This work was supported in part by a grant from the Naito Foundation.

Supporting information for this article is available on the WWW under http://dx.doi.org/10.1002/anie.200903183.

   

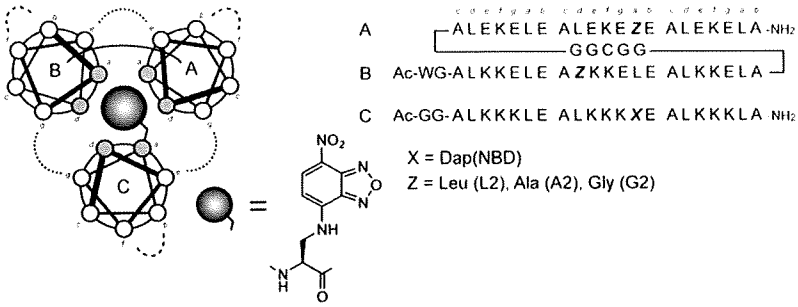


*Figure 1.* Structure and amino acid sequences of ZIP tag–probe pairs.

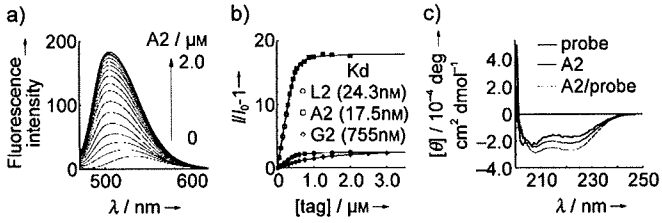


*Figure 2.* a) Fluorescence spectral change of the probe peptide upon addition of A2 at 25 °C in 50 mM 2-[4-(2-hydroxyethyl)piperazin-1-yl]ethanesulfonic acid (HEPES) buffer (pH 7.2, 100 mM NaCl): [probe] = 0.5 μM. b) Fluorescence titration curves of the probe peptide with L2, A2, and G2 at 516, 505, and 526 nm, respectively. $I$ and $I_0$ represent the fluorescence intensity at various concentrations of tag peptides and the initial fluorescence intensity, respectively. c) Circular dichroism spectra of the A2 tag (solid line), the probe peptide (bold line), and their complex (dashed line) at 25 °C in 50 mM Tris–HCl buffer (pH 7.2, 100 mM NaCl).

*Table 1:* Emission maxima [nm] and $\Delta I_{max}/I_0$ values (in parentheses) of the probe peptide and tag–probe complexes, dissociation constants ($K_d$) [nM] between the tag and probe peptides, and the α-helix contents [%] of the probe, the tag peptides, and their complexes (in parentheses).

| | Probe | L2 | A2 | G2 |
|---|---|---|---|---|
| $\lambda_{max}$ ($\Delta I_{max}/I_0$) | 536 (–) | 516 (2.7) | 505 (17.9) | 526 (2.5) |
| $K_d$[a] | – | 24.3 | 17.5 | 755 |
| α-helix content[b] | 53 | 81 (78) | 58 (71) | 18 (41) |

[a] Measurement conditions: 50 mM HEPES buffer solution (pH 7.2, 100 mM NaCl) at 25 °C, [probe] = 0.5 μM. [b] Measurement conditions: 50 mM Tris–HCl buffer solution (pH 7.2, 100 mM NaCl) at 25 °C; [tag], [probe], [tag–probe] = 1.0 μM. The α-helical contents were determined according to a standard method.[10]

wavelength shift and change in fluorescence intensity of the G2–probe pair were also small, which implies that the NBD moiety of the G2–probe peptide complex is located in a more hydrophilic area than those of the A2–probe peptide complex.

The dissociation constants of the probe peptide toward L2, A2, and G2 were estimated from the fluorescence titration curves by analysis with a nonlinear least-squares curve-fitting method[9] (Table 1). L2 and A2 showed high affinity, comparable to that of a normal antigen–antibody interaction, for the probe peptide. In general, the hydrophobicity of leucine zipper peptides is essential for their self-assembly and L2, for example, is more hydrophobic than A2 because it has two leucine residues. However, the binding affinity of the A2–probe pair is slightly superior to that of the L2–probe peptide pair, indicative not only of the hydrophobic interaction but also of the steric complementarity between A2 and the probe peptide, which is critical for the strong binding affinity. The binding affinity of G2 for the probe peptide is much lower than that of L2 or A2. Since a glycine residue generally destabilizes an α-helical structure, the structure of the G2–probe pair might be less stable than those of the L2– and A2–probe peptide pairs.

Circular dichroism (CD) spectra revealed that L2 and A2 tags, the probe peptide, and their complexes form α-helical structures (Figure 2c and Figure S3 in the Supporting Information). The probe peptide showed a CD spectral pattern typical of α-helical structures with negative maxima at 208 and 222 nm. L2, A2, and their complexes with the probe peptide also showed CD spectral patterns typical of α-helical structures. The α-helical content of A2 is lower than that of L2, which indicates that A2 forms a less stable α-helical structure than L2. However, the α-helix content of the A2–probe complex is higher than those of A2 or the probe peptides alone, which suggests that the A2–probe pair forms a stable 3α-helical bundle structure. Furthermore, the enhanced α-helical structure of the A2–probe complex is nearly equal to that in the L2–probe complex, which indicates that A2 can form a stable 3α-helical leucine zipper structure with the probe peptide. The CD spectrum of G2, however, shows a random-coil pattern and the α-helix content of the G2–probe complex is only 41 %. These results imply that the mutation of the leucine or alanine residues to glycine causes the destabilization of the structure of G2 and of the G2–probe complex, and it is thought that this is the reason why the G2–probe pair has a lower binding affinity than the A2–probe pair.

The fluorescence titration experiment and the CD spectra suggest that formation of a stable α-helical structure with a hydrophobic pocket is necessary for high binding affinity and fluorogenic activity. A2 forms a stable α-helical structure with a pocket that can accommodate NBD and it is thought, therefore, that the combination of the A2 tag and the probe leads to expression of the remarkable fluorescence activity. In addition, the A2–probe pair showed the same fluorescence spectral change in the cell lysate solution (Figure S7 in the Supporting Information), thus indicating that A2 is the most appropriate partner of the probe peptide as a fluorogenic tag–probe pair for protein imaging in vivo.

Next, we investigated whether our ZIP tag–probe system is available for the fluorescence imaging of proteins in living cells. CXCR4 was chosen as a model protein. CXCR4 is one of the 7-transmembrane G-protein coupled receptors, a member of a chemokine receptor family.[11] The A2 tag is genetically fused at the N terminus of CXCR4, which is an extracellular region, through the $(Gly\text{-}Ser)_6$ linker sequence. The A2-tag-fused CXCR4 is transiently expressed on the surface of Chinese hamster ovary K1 (CHO-K1) cells, and double labeling experiments of the A2-tag-fused CXCR4 using a fluorescent CXCR4 antagonist with tetramethylrhod-

  

amine (TAMRA)[12] and the probe peptide with the NBD dye were performed. The A2-tag-fused CXCR4 was specifically stained with red fluorescence by TAMRA-appended CXCR4 antagonist (Figure S8a in the Supporting Information). Then, the sequential labeling of the A2-tag-fused CXCR4 was performed using the probe peptide. Before removal of the probe peptide, a bright green fluorescence was observed on the surface of cells in the presence of excess probe peptide, but the fluorescence resulting from this peptide was not observed in CHO-K1 cells without expression of the A2-tag-fused CXCR4 (Figure 3b). Fluorescence arising from the TAMRA-appended CXCR4 antagonist was also observed (Figure 3a), which suggests that the binding events between the A2 tag and the probe peptide, and between CXCR4 and the TAMRA-appended CXCR4 antagonist, are independent of each other. The fluorescence image derived from the probe peptide was merged well with the fluorescence image of the TAMRA-appended CXCR4 antagonist (Figure 3c,d). After removal of the probe peptide by the exchange of culture medium, similar fluorescence images were also observed (Figure S9 in the Supporting Information). These results suggest that CXCR4 can be successfully visualized using our ZIP tag–probe system without removal of excess probe molecules. This ZIP tag–probe system is consequently a useful fluorescence-imaging tool for proteins in living cells.

In conclusion, we have developed a new functional peptide pair with fluorogenic activity based on leucine zipper peptides. The alanine-substituted tag peptide A2 binds strongly to a probe peptide, and this binding is accompanied by a dramatic fluorescent colorimetric change from weak yellow to bright green. In addition, we have demonstrated that the fluorescence imaging of A2-tag-fused CXCR4, which is a membrane-bound protein, is successfully achieved by the probe peptide. Recently, Yano et al. reported that two α-helical leucine zipper tag–probe pairs are useful fluorescence imaging tools for membrane-bound proteins.[13]

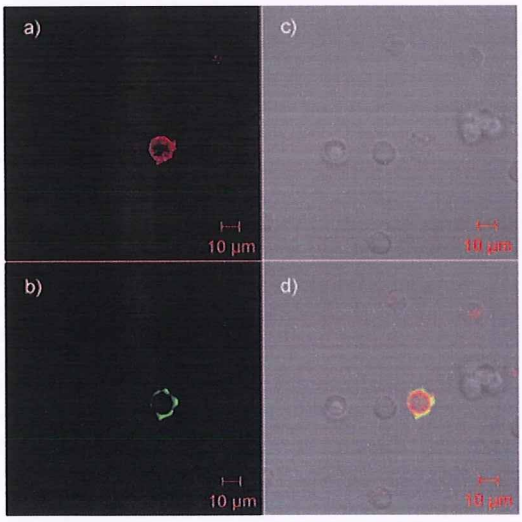


***Figure 3.*** Sequential labeling of A2-tag-fused CXCR4 by the probe peptide after labeling by TAMRA-appended CXCR4 antagonist. a) Fluorescence image derived from TAMRA (excitation: 543 nm, emission filter: > 560 nm). b) Fluorescence image derived from NBD (excitation: 458 nm, emission filter: 505–530 nm). c) Differential interference contrast. d) Merged image of (a)–(c).

Our ZIP tag–probe pairs have, in addition, fluorogenic activity which might facilitate the real-time imaging of proteins without the necessity to remove excess probe molecules. Thus, ZIP tag–probe pairs would become valuable imaging tools for target proteins in living cells.

Received: June 12, 2009
Revised: September 24, 2009
Published online: October 28, 2009

**Keywords:** fluorescent probes · imaging · living cells · peptides · proteins

[1] a) K. Terpe, *Appl. Microbiol. Biotechnol.* **2003**, *60*, 523–533; b) M. Hedhammar, T. Gräslund, S. Hober, *Chem. Eng. Technol.* **2005**, *28*, 1315–1325; c) E. G. Guignet, R. Hovius, H. Vogel, *Nat. Biotechnol.* **2004**, *22*, 440–444; d) C. R. Goldsmith, J. Jaworski, M. Sheng, S. J. Lippard, *J. Am. Chem. Soc.* **2006**, *128*, 418–419; e) C. T. Hauser, R. Y. Tsien, *Proc. Natl. Acad. Sci. USA* **2007**, *104*, 3693–3697.

[2] a) B. A. Griffin, S. R. Adams, R. Y. Tsien, *Science* **1998**, *281*, 269–272; b) G. Gaietta, T. J. Deerinck, S. R. Adams, J. Bouwer, O. Tour, D. W. Laird, G. E. Sosinsky, R. Y. Tsien, M. H. Ellisman, *Science* **2002**, *296*, 503–507.

[3] a) K. M. Marks, M. Rosinov, G. P. Nolan, *Chem. Biol.* **2004**, *11*, 347–356; b) A. Ojida, K. Honda, D. Shinmi, S. Kiyonaka, Y. Mori, I. Hamachi, *J. Am. Chem. Soc.* **2006**, *128*, 10452–10459; c) I. Chen, Y.-A. Choi, A. Y. Ting, *J. Am. Chem. Soc.* **2007**, *129*, 6619–6625; d) H. M. O'Hare, K. Johnsson, A. Gautier, *Curr. Opin. Struct. Biol.* **2007**, *17*, 488–494.

[4] a) A. Keppler, S. Gendreizig, T. Gronemeyer, H. Pick, K. Johnsson, *Nat. Biotechnol.* **2003**, *21*, 86–89; b) A. Gautier, A. Juillerat, C. Heinis, I. R. Corrêa, Jr., M. Kindermann, F. Beaufils, K. Johnsson, *Chem. Biol.* **2008**, *15*, 128–136; c) J. Yin, F. Liu, X. Li, C. T. Walsh, *J. Am. Chem. Soc.* **2004**, *126*, 7754–7755; d) G. V. Los, A. Darzins, N. Karassina, C. Zimprich, R. Learish, M. G. McDougall, L. P. Encell, R. Friedman-Ohana, M. Wood, G. Vidurgiris et al., *Promega Cell Notes* **2005**, *11*, 2–6.

[5] a) B. Tripet, L. Yu, D. L. Bautista, W. Y. Wong, R. T. Irvin, R. S. Hodges, *Protein Eng.* **1996**, *9*, 1029–1042; b) K. Zhang, M. R. Diehl, D. A. Tirrell, *J. Am. Chem. Soc.* **2005**, *127*, 10136–10137; c) S. Yuzawa, T. Mizuno, T. Tanaka, *Chem. Eur. J.* **2006**, *12*, 7345–7352.

[6] a) I. Obataya, S. Sakamoto, A. Ueno, H. Mihara, *Biopolymers* **2001**, *59*, 65–71; b) M. K. Yadav, J. E. Redman, L. J. Leman, J. M. Alvarez-Gutiérrez, Y. Zhang, C. D. Stout, M. R. Ghadiri, *Biochemistry* **2005**, *44*, 9723–9732.

[7] B. Lovejoy, S. Choe, D. Cascio, D. K. McRorie, W. F. DeGrado, D. Eisenberg, *Science* **1993**, *259*, 1288–1293.

[8] S. Uchiyama, T. Santa, K. Imai, *J. Chem. Soc. Perkin Trans. 2* **1999**, 2525–2532.

[9] T. Kuwabara, A. Nakamura, A. Ueno, F. Toda, *J. Phys. Chem.* **1994**, *98*, 6297–6303.

[10] a) Y.-H. Chen, J. T. Yang, K. H. Chau, *Biochemistry* **1974**, *13*, 3350–3359; b) P. J. Gans, P. C. Lyu, M. C. Manning, R. W. Woody, N. R. Kallenbach, *Biopolymers* **1991**, *31*, 1605–1614; c) D. Y. Jackson, D. S. King, J. Chmielewski, S. Singh, P. G. Schultz, *J. Am. Chem. Soc.* **1991**, *113*, 9391–9392.

[11] a) S. G. Ward, J. Westwick, *Biochem. J.* **1998**, *333*, 457–470; b) H. Tamamura, H. Tsutsumi, W. Nomura, T. Tanaka, N. Fujii, *Expert Opin. Drug Discovery* **2008**, *3*, 1155–1166.

[12] W. Nomura, Y. Tanabe, H. Tsutsumi, T. Tanaka, K. Ohba, N. Yamamoto, H. Tamamura, *Bioconjugate Chem.* **2008**, *19*, 1917–1920.

[13] Y. Yano, A. Yano, S. Oishi, Y. Sugimoto, G. Tsujimoto, N. Fujii, K. Matsuzaki, *ACS Chem. Biol.* **2008**, *3*, 341–345.

  

Bioorganic & Medicinal Chemistry Letters 20 (2010) 354–358

Contents lists available at ScienceDirect

Bioorganic & Medicinal Chemistry Letters

journal homepage: www.elsevier.com/locate/bmcl

# CD4 mimics targeting the mechanism of HIV entry

Yuko Yamada [a], Chihiro Ochiai [a], Kazuhisa Yoshimura [b], Tomohiro Tanaka [a], Nami Ohashi [a], Tetsuo Narumi [a], Wataru Nomura [a], Shigeyoshi Harada [b], Shuzo Matsushita [b], Hirokazu Tamamura [a,*]

[a] Institute of Biomaterials and Bioengineering, Tokyo Medical and Dental University, Chiyoda-ku, Tokyo 101-0062, Japan
[b] Center for AIDS Research, Kumamoto University, Kumamoto 860-0811, Japan

ARTICLE INFO

*Article history:*
Received 19 September 2009
Revised 20 October 2009
Accepted 22 October 2009
Available online 4 November 2009

*Keywords:*
CD4 mimic
HIV entry
Synergistic effect
CXCR4

ABSTRACT

A structure–activity relationship study was conducted of several CD4 mimicking small molecules which block the interaction between HIV-1 gp120 and CD4. These CD4 mimics induce a conformational change in gp120, exposing its co-receptor-binding site. This induces a highly synergistic interaction in the use in combination with a co-receptor CXCR4 antagonist and reveals a pronounced effect on the dynamic supramolecular mechanism of HIV-1 entry.



Recently, remarkable success has attended the clinical treatment of HIV-infected and AIDS patients, with 'highly active antiretroviral therapy (HAART)'. This approach involves a combination of two or three agents from two categories: reverse transcriptase inhibitors and protease inhibitors.[1] In addition, the molecular mechanism involved in HIV-entry and -fusion into host cells has been described in detail.[2] The complex interactions of surface proteins on cellular and viral membranes, which are designated as a dynamic supramolecular mechanism of HIV entry, are reported to be crucial to the viral infection. In a first step, an HIV envelope protein, gp120 interacts with a cell surface protein, CD4, leading to a conformational change in gp120 followed by subsequent binding of gp120 to a co-receptor CCR5[3] or CXCR4.[4] CCR5 and CXCR4 are the major co-receptors for the entry of macrophage-tropic (R5-) and T cell line-tropic (X4-) HIV-1, respectively. The interaction of gp120 with CCR5 or CXCR4 triggers entry of another envelope protein, gp41 to the cell membrane and formation of a gp41 trimer-of-hairpins structure, which causes fusion of HIV/cell-membranes and completes the infection.

Informed by this mechanism, a fusion inhibitor, enfuvirtide (fuzeon, Trimers & Roche)[5] and a CCR5 antagonist, maraviroc (Pfizer)[6] in addition to an integrase inhibitor, raltegravir (Merck)[7] have been used clinically. However, serious problems with chemotherapy still persist, including the emergence of viral strains with multi-drug resistance (MDR), considerable adverse effects and high costs. Consequently, development of novel drugs possessing mechanisms of action different from those of the above inhibitors is currently required. We have previously developed selective CXCR4 antagonists[8] and fusion inhibitors.[9] Furthermore, *N*-(4-Bromophenyl)-*N*′-(2,2,6,6-tetramethylpiperidin-4-yl)-oxalamide (**1**) and *N*-(4-chlorophenyl)-*N*′-(2,2,6,6-tetramethylpiperidin-4-yl)-oxalamide (**2**) were previously found using chemical library screening to inhibit syncytium formation by other researchers.[10] **1** and **2** bind to gp120 with binding affinities of $K_d$ = 2.2 μM and 3.7 μM, respectively, blocking the interaction of gp120 with CD4 in the first step of an HIV-1 entry. Thus, in the present study we focus on the development of CD4 mimics that can block the interaction between gp120 and CD4. We have investigated the effect of CD4 mimics on conformational changes of gp120 and on their use in combination use with a CXCR4 antagonist.

Initially, molecular modeling of compound **2** docked into gp120 was carried out using docking simulations performed by the FlexSIS module of SYBYL 7.1 (Tripos, St. Louis) (Fig. 1).[11] The atomic coordinates of the crystal structure of gp120 with soluble CD4 (sCD4) were retrieved from Protein Data Bank (PDB) (entry 1RZJ) (Fig. 1a) and it was observed that $Phe^{43}$ and $Arg^{59}$ of the CD4 have multiple contacts with $Asp^{368}$, $Glu^{370}$ and $Trp^{427}$ of gp120, which are all conserved residues. An inspection of the environment of compound **2** docked in gp120 revealed the presence of a large cavity around the *p*-position of the phenyl ring of compound **2**, which could interact with the viral surface protein gp120 (Fig. 1b and c). Several analogs of **2** with substituents on the phenyl ring were therefore synthesized.

All compounds except **12** were synthesized by previously published methods (Scheme 1).[10b,12,13] Aniline derivatives (**3**) were coupled with ethyl oxalyl chloride to yield the corresponding ethyl oxalamates **4**. Saponification of the above oxalamates to the corresponding free acids and the subsequent coupling with 4-ami-

* Corresponding author.
*E-mail address:* tamamura.mr@tmd.ac.jp (H. Tamamura).

0960-894X/$ - see front matter © 2009 Elsevier Ltd. All rights reserved.
doi:10.1016/j.bmcl.2009.10.098

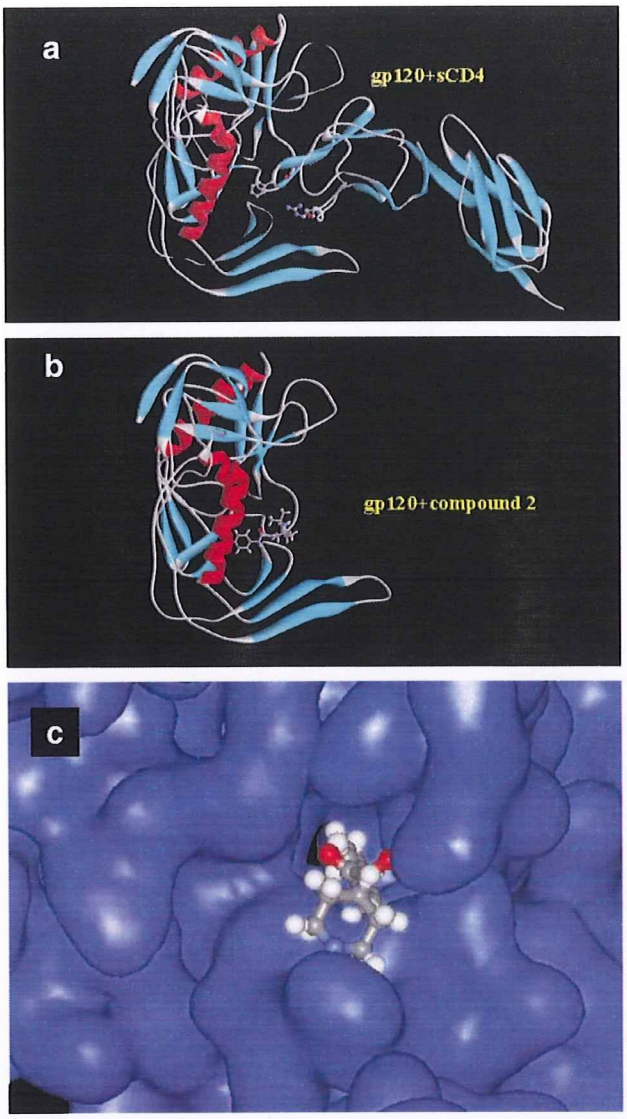


**Figure 1.** (a) The crystal structure of gp120 with soluble CD4 (sCD4) retrieved from the PDB (entry 1RZJ); (b) docking structure of compound **2** and gp120; (c) a focused figure of (b) shown by space-filling model.

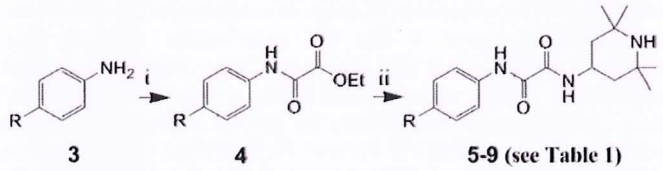


**Scheme 1.** Reagents and conditions: (i) ethyl oxalyl chloride, $Et_3N$; (ii) 1 M NaOH; 4-amino-2,2,6,6-tetramethylpiperidine, 1-(3-dimethylaminopropyl)-3-ethylcarbodiimide hydrochloride, 1-hydroxybenzotriazole, $Et_3N$.

no-2,2,6,6-tetramethylpiperidine using 1-ethyl-3-(3-dimethylaminopropyl)carbodiimide hydrochloride (EDC) and 1-hydroxybenzotriazole (HOBt) yielded compounds **5–9**. In the case of compound **12**, whose amide bond is not stable during the reaction of the saponification of the corresponding oxalamates, an alternative synthetic scheme was used (Scheme 2).[14] The reaction of *p*-nitroaniline (**10**) with oxalyl chloride gave the corresponding oxoacetamide **11**, which was subsequently coupled with 4-amino-2,2,6,6-tetramethylpiperidine to yield the desired compound **12**.

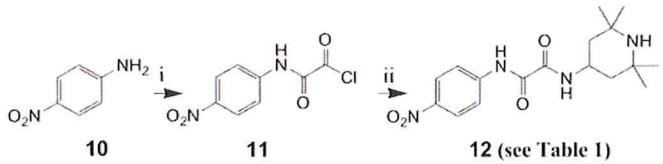


**Scheme 2.** Reagents and conditions: (i) oxalyl chloride, $Et_3N$; (ii) 4-amino-2,2,6,6-tetramethylpiperidine, $Et_3N$.

The anti-HIV activity of the synthetic compounds was evaluated against various viral strains including both laboratory and primary isolates (Table 1). $IC_{50}$ values were determined by the 3-(4,5-dimethylthiazol-2-yl)-2,5-diphenyltetrazolium bromide (MTT) method[15] as the concentrations of the compounds which conferred 50% protection against HIV-1-induced cytopathogenicity in PM1/CCR5 cells. Cytotoxicity of the compounds based on the viability of mock-infected PM1/CCR5 cells was also evaluated using the MTT method. $CC_{50}$ values were determined as the concentrations achieving 50% reduction of the viability of mock-infected cells. Compounds **1** and **2** showed potent anti-HIV activity against laboratory isolates, IIIB (X4, Sub B) and 89.6 (dual, Sub B) strains, and compound **2** also possessed potent activity against a primary isolate, an fTOI strain (R5, Sub B). All of the $IC_{50}$ values were between 4 μM and 10 μM. Compound **1** was not tested against primary isolates. The potencies of compounds **1** and **2** are comparable to the reported binding affinities for gp120 ($K_d$ = 2.2 and 3.7 μM, respectively).[10] Several of the new analogs of compounds **1** and **2** showed significant anti-HIV activity. Compound **5**, which has a phenyl group in place of the *p*-chlorophenyl group of compound **2**, did not show significant anti-HIV activity at concentrations below 100 μM against all strains tested except for an fTOI strain (R5, Sub B). This result suggests that a substituent at the *p*-position of the phenyl ring is critical for potent activity. Compound **6**, which has a fluorine atom at the *p*-position of the phenyl ring, showed moderate anti-HIV activity against laboratory isolates, IIIB (X4, Sub B) and 89.6 (dual, Sub B) strains ($IC_{50}$ = 61 and 81 μM, respectively), but, at concentrations below 100 μM, failed to show significant anti-HIV activity against a primary isolate, a KYAG strain (R5, Sub B). Among halogen atoms, fluorine is less suitable than bromine or chlorine as a substituent at the *p*-position of the phenyl ring, as evidenced by compound **6**, which is 8–15-fold less potent than compounds **1** and **2** against IIIB (X4, Sub B) and 89.6 (dual, Sub B) strains. Compound **7**, which has a methyl group at the *p*-position of the phenyl ring, showed relatively more potent activity against IIIB (X4, Sub B) and 89.6 (dual, Sub B) strains ($IC_{50}$ = 23 and 41 μM, respectively) than compound **6**. Compound **7** also showed significant anti-HIV activity against primary isolates, fTOI (R5, Sub B) and KYAG (R5, Sub B) strains ($IC_{50}$ = 16 and 51 μM, respectively). Compound **8**, with a methoxy group at the *p*-position of the phenyl ring, did not show significant anti-HIV activity against all strains tested until a concentration of 100 μM was reached. In the biological assays, derivatives having electron-withdrawing substituents such as bromine, chlorine and fluorine at the *p*-position of the phenyl ring are relatively potent, whereas derivatives having electron-donating groups such as methoxy at this position are not potent. Furthermore, the steric effect of a substituent at the *p*-position of the phenyl ring appears to be critical to anti-HIV activity. The sum of Hammett constants ($\sigma$) of benzoic acid substituents[16] shown in Table 1 can be used to evaluate the electron-withdrawing or -donating effect of the substituents on the aromatic ring. The Taft $E_s$ values[16a,17] were used as steric parameters for substituents at the *p*-position of the phenyl ring. The order of potency found for the halogen-containing derivatives in anti-HIV activity against laboratory isolates, IIIB (X4, Sub B) and 89.6 (dual, Sub B), is: compound **1** (R = Br) ($\sigma$ = 0.23, $E_s$ = −1.16), **2**

**Table 1**
Hammett constants ($\sigma$) and steric effects ($E_s$) of substituted aromatic rings and anti-HIV activity and cytotoxicity of synthetic compounds

| Compd | R[a] | $\sigma$[b] | $E_s$[c] | $IC_{50}$[e] (μM) | | | | $CC_{50}$[e] (μM) |
|---|---|---|---|---|---|---|---|---|
| | | | | Lab. isolates | | Primary isolates | | |
| | | | | IIIB (X4) | 89.6 (dual) | fTOI (R5) | KYAG (R5) | |
| **1** | Br | 0.23 | −1.16 | 4 | 9 | ND | ND | 150 |
| **2** | Cl | 0.23 | −0.97 | 8 | 10 | 5 | >30 | 170 |
| **5** | H | 0 | 0 | >100 | >100 | 81 | >100 | 350 |
| **6** | F | 0.06 | −0.46 | 61 | 81 | ND | >100 | 320 |
| **7** | $CH_3$ | −0.17 | −1.24 | 23 | 41 | 16 | 51 | 210 |
| **8** | $OCH_3$ | −0.27 | −0.55 | >100 | >100 | ND | >100 | 340 |
| **9** | $CF_3$ | 0.54 | −2.40 | ND | 27 | ND | ND | 72 |
| **12** | $NO_2$ | 0.78 | −1.77[d] | ND | 42 | ND | ND | 230 |
| sCD4 | | | | 0.010 | 0.021 | 0.0044 | ND | ND |

[a] See Schemes 1 and 2.
[b] $\sigma$ = Hammett constant of a substitutent on a benzoic acid derivative.[16]
[c] $E_s$ = steric effect of a substituent at the *para* position on the aromatic ring.[16a,17]
[d] The average value of −1.01 and −2.52, which are $E_s$ values of the $NO_2$ group, −1.77, was used.
[e] Values are means of at least three experiments (ND = not determined).

(R = Cl) ($\sigma$ = 0.23, $E_s$ = −0.97), **6** (R = F) ($\sigma$ = 0.06, $E_s$ = −0.46) and **5** (R = H) ($\sigma$ = 0, $E_s$ = 0). This is the order of substituents' electron-withdrawing ability and also of their size. Methyl ($\sigma$ = −0.17, $E_s$ = −1.24) is an electron-donating group, but is almost as bulky as a bromine atom. Thus, the *p*-methyl derivative **7** has relatively potent anti-HIV activity against laboratory isolates, IIIB (X4, Sub B) and 89.6 (dual, Sub B), higher than that of compound **6** (R = F) but lower than that of compound **1** (R = Br) or **2** (R = Cl). The electron-donating ability of a methoxy group is stronger ($\sigma$ = −0.27), but the bulk size is smaller ($E_s$ = −0.55), than that of a methyl group. Thus, the *p*-methoxy derivative **8** has no significant anti-HIV activity against all strains tested at concentrations below 100 μM. Two derivatives containing bulkier and more potent electron-withdrawing substituents such as trifluoromethyl (R = $CF_3$) ($\sigma$ = 0.54, $E_s$ = −2.40) and nitro (R = $NO_2$) ($\sigma$ = 0.78, $E_s$ = −1.77) at the *p*-position of the phenyl ring were evaluated. Compounds **9** (R = $CF_3$) and **12** (R = $NO_2$) showed significant anti-HIV activity against an 89.6 (dual, Sub B) strain. These are less potent than compounds **1** and **2** and this is perhaps due to the excessive size of the substituents at the *p*-position. This suggests that a certain level of the bulk size and a potent electron-withdrawing ability of the substituents are preferable for anti-HIV activity. It is estimated that a cavity around the *p*-position of the phenyl ring of CD4 mimicking compounds would be optimally filled by bromine ($E_s$ = −1.16) or a methyl group ($E_s$ = −1.24) at *p*-position, and that an electron-deficient aromatic ring might interact tightly with a negatively charged group such as carboxy of $Glu^{370}$. In isothermal titration calorimetry (ITC) experiments reported elsewhere,[10c] compound **5** (R = H) does not have significant affinity for gp120, and compound **6** (R = F) has less potent affinity for gp120 than compound **2**, consistent with the present data. In all but one of the compounds, no significant cytotoxicity was detected ($CC_{50}$ >150 μM, Table 1), the exception being compound **9** (R = $CF_3$) ($CC_{50}$ = 72 μM). Compounds **7** and **12** have relatively low cytotoxicities, compared to compounds **1** and **2**.

Fluorescence activated cell sorting (FACS) analysis was performed[15] to investigate whether these synthetic compounds interact with gp120 inducing the conformational change necessary for the approach of an anti-envelope antibody or a co-receptor to the gp120. The profile of binding of an anti-envelope CD4-induced monoclonal antibody, 4C11, to the Env-expressing cell surface (an R5-HIV-1 strain, JR-FL,-infected PM1 cells) pretreated with the above CD4 mimic analogs was examined. Comparison of the binding of 4C11 to the cell surface was measured in terms of the mean fluorescence intensity (MFI), and is shown in Figure 2. Pretreatment of the Env-expressing cells with compound **2** (MFI = 38.42) produced a remarkable increase in binding affinity for 4C11, similar to that observed in pretreatment with sCD4 (MFI = 37.90). This is consistent with the results in the previous paper[10] where it was reported that compound **2** enhances the binding of gp120 to the 17b monoclonal antibody which recognizes the co-receptor binding site of gp120. Env-expressing cells, which were not pretreated with sCD4 or a CD4 mimic compound, did not show significant binding affinity for 4C11 (Fig. 2, blank). The increase in binding affinity for monoclonal antibodies may be due to conformational changes in gp120, which were caused by the interaction of sCD4 or a CD4 mimic with gp120. It is hypothesized that such conformational changes involve the exposure of the co-receptor binding site of gp120 (the V3 loop), which is hidden internally, since the binding of gp120 to 17b is enhanced. Compound **5**, which failed to show significant anti-HIV activity, and compounds **7**, **9** and **12**, which had significant anti-HIV activity, were assessed in the FACS analysis. The profile of the binding of 4C11 to the Env-expressing cell surface pretreated with compound **5** (MFI = 14.34) was similar to that of the blank (MFI = 11.24), suggesting that compound **5** offers no significant enhancement of binding affinity for 4C11. This result is compatible with the anti-HIV activity of compound **5**. The profile of the binding of 4C11 to the Env-expressing cell surface pretreated with compound **7** (MFI = 38.33) was entirely similar to that of compound **2** used as a pretreatment. Pretreatment of the cell surface with compounds **9** and **12** (MFI = 29.09 and 30.01, respectively) produced a slightly lower enhancement of binding affinity for 4C11, compared to those of compounds **2** and **7** as pretreatments. However, in the ITC experiments reported elsewhere,[10c] compound **9** (R = $CF_3$) has a high affinity for gp120, comparable to that of compound **2**, but compound **12** (R = $NO_2$) does not have significant affinity for gp120, indicating that these are not consistent with the current FACS studies, possibly due to the difference in the assay systems. Although the anti-HIV activity of **7** is weaker than that of compound **2**, the level of compound **7** inducing an enhancement of binding affinity of gp120 for 4C11 is comparable to that of compound **2**. The concentration of compounds used in the FACS analysis was 100 μM, much beyond the $IC_{50}$ values of compounds **2** and **7**. A concentration of 100 μM would be also sufficient for the expression of anti-HIV activity caused by compounds **2** and **7**.

An effect on the use of compound **2** combined with another entry inhibitor was investigated. Analysis of the synergistic effects of anti-HIV agents was performed according to the median effect principle using the CalcuSyn version 2 computer program[18] to estimate $IC_{50}$ values of compounds in different combinations. Combination indices (CI) were estimated from the data evaluated using the MTT assay

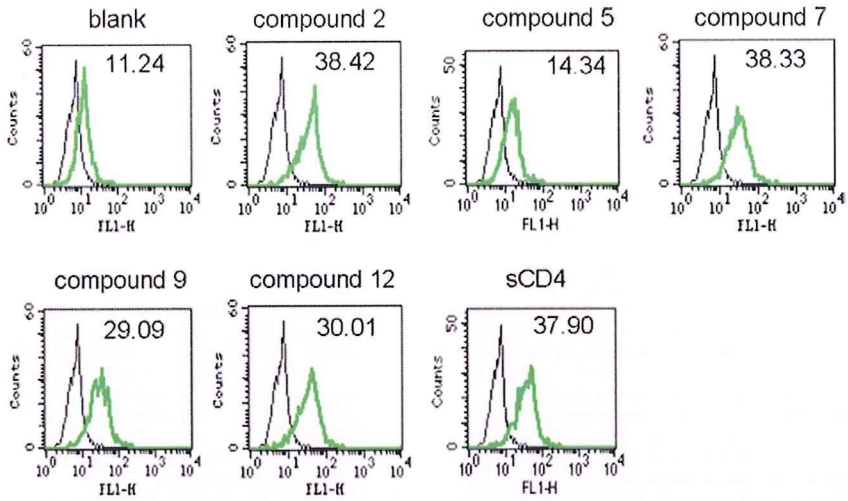


**Figure 2.** JR-FL (R5, Sub B) chronically infected PM1 cells were preincubated with 100 μM of a CD4 mimic or sCD4 (11 nM) for 15 min, and then incubated with an anti-HIV-1 mAb, 4C11, at 4 °C for 15 min. The cells were washed with PBS, and fluorescein isothiocyanate (FITC)-conjugated goat anti-human IgG antibody was used for antibody-staining. Flow cytometry data for the binding of 4C11 (green lines) to the Env-expressing cell surface in the presence of sCD4 or a CD4 mimic are shown among gated PM1 cells along with a control antibody (anti-human CD19: black lines). Data are representative of the results from a minimum of two independent experiments. The number at the top of each graph shows the mean fluorescence intensity (MFI) of the antibody 4C11.

**Table 2**
Combination indices (CI) for compound **2** or sCD4 and a CXCR4 antagonist, T140, against an HIV IIIB strain

| Combination | HIV strain | CI values at different IC[a] | | |
|---|---|---|---|---|
| | | $IC_{50}$ | $IC_{75}$ | $IC_{90}$ |
| 2 + T140 | IIIB | 0.786 | 0.713 | 0.655 |
| sCD4 + T140 | IIIB | 0.705 | 0.528 | 0.400 |

[a] The multiple-drug effect analysis reported by Chou et al. was used to analyze the effects of combinational uses of compounds.[18] CI <0.9: synergy, 0.9 < CI < 1.1: additivity, CI >1.1: antagonism.

(Table 2).[15] Compound **2** showed a highly remarkable synergistic anti-HIV activity with a co-receptor CXCR4 antagonist, T140,[8a] against an X4-HIV-1 strain, IIIB at various IC values ($IC_{50}$, $IC_{75}$ and $IC_{90}$). However, sCD4 exhibited a higher synergistic effect (lower CI values) with T140 (Table 2). The interaction of sCD4 or a CD4 mimic with gp120 would expose the co-receptor-binding site of gp120, and the co-receptor CXCR4 could then easily approach gp120. Thus, an inhibitory effect of a CXCR4 antagonist would be meaningful, and a significant synergistic effect might also be brought about by a combination of sCD4 or a CD4 mimic and T140.

In summary, a series of CD4 mimic compounds were synthesized and evaluated for their anti-HIV activity. Several compounds showed significant anti-HIV activity with relatively low cytotoxicity. SAR studies showed that a certain level of size and electron-withdrawing ability of the substituents at the *p*-position of the phenyl ring are suitable for potent anti-HIV activity. In addition, the treatment of Env-expressing cells with several CD4 mimicking compounds causes a conformational change, exposing the co-receptor-binding site of gp120 externally. Thus, a CD4 mimic exhibited a remarkable synergistic effect with a co-receptor antagonist. These compounds are essential probes directed to the dynamic supramolecular mechanism of HIV entry, and important leads for the cocktail therapy of AIDS.

## Acknowledgments

This work was supported by Mitsui Life Social Welfare Foundation, Grant-in-Aid for Scientific Research from the Ministry of Education, Culture, Sports, Science, and Technology of Japan, and Health and Labour Sciences Research Grants from Japanese Ministry of Health, Labor, and Welfare.

## References and notes

1. Mitsuya, H.; Erickson, J. In *Textbook of AIDS Medicine*; Merigan, T. C., Bartlett, J. G., Bolognesi, D., Eds.; Williams & Wilkins: Baltimore, 1999; pp 751–780.
2. Chan, D. C.; Kim, P. S. *Cell* **1998**, *93*, 681.
3. (a) Alkhatib, G.; Combadiere, C.; Broder, C. C.; Feng, Y.; Kennedy, P. E.; Murphy, P. M.; Berger, E. A. *Science* **1996**, *272*, 1955; (b) Choe, H.; Farzan, M.; Sun, Y.; Sullivan, N.; Rollins, B.; Ponath, P. D.; Wu, L.; Mackay, C. R.; LaRosa, G.; Newman, W.; Gerard, N.; Gerard, C.; Sodroski, J. *Cell* **1996**, *85*, 1135; (c) Deng, H. K.; Liu, R.; Ellmeier, W.; Choe, S.; Unutmaz, D.; Burkhart, M.; Marzio, P. D.; Marmon, S.; Sutton, R. E.; Hill, C. M.; Davis, C. B.; Peiper, S. C.; Schall, T. J.; Littman, D. R.; Landau, N. R. *Nature* **1996**, *381*, 661; (d) Doranz, B. J.; Rucker, J.; Yi, Y. J.; Smyth, R. J.; Samson, M.; Peiper, S. C.; Parmentier, M.; Collman, R. G.; Doms, R. W. *Cell* **1996**, *85*, 1149; (e) Dragic, T.; Litwin, V.; Allaway, G. P.; Martin, S. R.; Huang, Y.; Nagashima, K. A.; Cayanan, C.; Maddon, P. J.; Koup, R. A.; Moore, J. P.; Paxton, W. A. *Nature* **1996**, *381*, 667.
4. Feng, Y.; Broder, C. C.; Kennedy, P. E.; Berger, E. A. *Science* **1996**, *272*, 872.
5. Wild, C. T.; Greenwell, T. K.; Matthews, T. J. *AIDS Res. Hum. Retroviruses* **1993**, *9*, 1051.
6. (a) Dorr, P.; Westby, M.; Dobbs, S.; Griffin, P.; Irvine, B.; Macartney, M.; Mori, J.; Rickett, G.; Smith-Burchnell, C.; Napier, C.; Webster, R.; Armour, D.; Price, D.; Stammen, B.; Wood, A.; Perros, M. *Antimicrob. Agents Chemother.* **2005**, *49*, 4721; (b) Price, D. A.; Armour, D.; De Groot, M.; Leishman, D.; Napier, C.; Perros, M.; Stammen, B. L.; Wood, A. *Bioorg. Med. Chem. Lett.* **2006**, *16*, 4633.
7. (a) Cahn, P.; Sued, O. *Lancet* **2007**, *369*, 1235; (b) Grinsztejn, B.; Nguyen, B.-Y.; Katlama, C.; Gatell, J. M.; Lazzarin, A.; Vittecoq, D.; Gonzalez, C. J.; Chen, J.; Harvey, C. M.; Isaacs, R. D. *Lancet* **2007**, *369*, 1261.
8. (a) Tamamura, H.; Xu, Y.; Hattori, T.; Zhang, X.; Arakaki, R.; Kanbara, K.; Omagari, A.; Otaka, A.; Ibuka, T.; Yamamoto, N.; Nakashima, H.; Fujii, N. *Biochem. Biophys. Res. Commun.* **1998**, *253*, 877; (b) Fujii, N.; Oishi, S.; Hiramatsu, K.; Araki, T.; Ueda, S.; Tamamura, H.; Otaka, A.; Kusano, S.; Terakubo, S.; Nakashima, H.; Broach, J. A.; Trent, J. O.; Wang, Z.; Peiper, S. C. *Angew. Chem., Int. Ed.* **2003**, *42*, 3251; (c) Tanaka, T.; Nomura, W.; Narumi, T.; Esaka, A.; Oishi, S.; Ohashi, N.; Itotani, K.; Evans, B. J.; Wang, Z.; Peiper, S. C.; Fujii, N.; Tamamura, H. *Org. Biomol. Chem.* **2009**, *7*, 3805.
9. Otaka, A.; Nakamura, M.; Nameki, D.; Kodama, E.; Uchiyama, S.; Nakamura, S.; Nakano, H.; Tamamura, H.; Kobayashi, Y.; Matsuoka, M.; Fujii, N. *Angew. Chem., Int. Ed.* **2002**, *41*, 2937.
10. (a) Zhao, Q.; Ma, L.; Jiang, S.; Lu, H.; Liu, S.; He, Y.; Strick, N.; Neamati, N.; Debnath, A. K. *Virology* **2005**, *339*, 213; (b) Schön, A.; Madani, N.; Klein, J. C.; Hubicki, A.; Ng, D.; Yang, X.; Smith, A. B., III; Sodroski, J.; Freire, E. *Biochemistry* **2006**, *45*, 10973; (c) Madani, N.; Schön, A.; Princiotto, A. M.; LaLonde, J. M.; Courter, J. R.; Soeta, T.; Ng, D.; Wang, L.; Brower, E. T.; Xiang, S.-H.; Do Kwon, Y.; Huang, C.-C.; Wyatt, R.; Kwong, P. D.; Freire, E.; Smith, A. B., III; Sodroski, J. *Structure* **2008**, *16*, 1689; (d) Haim, H.; Si, Z.; Madani, N.; Wang, L.; Courter, J. R.; Princiotto, A.; Kassa, A.; DeGrace, M.; McGee-Estrada, K.; Mefford, M.; Gabuzda, D.; Smith, A. B., III; Sodroski, J. *ProS Pathogens* **2009**, *5*, 1.
11. The structure of compound **2** was built in Sybyl and minimized with the MMFF94 force field and partial charges. (see: Halgren, T. A. *J. Comput. Chem.* **1996**, *17*, 490.) Docking was then performed using FlexSIS through its SYBYL

module, into the crystal structure of gp120 (PDB, entry 1RZJ). The binding site was defined as residues $Val^{255}$, $Asp^{368}$, $Glu^{370}$, $Ser^{375}$, $Ile^{424}$, $Trp^{427}$, $Val^{430}$ and $Val^{475}$, and included residues located within a radius 4.4 Å. The ligand was considered to be flexible, and all other options were set to their default values. Figures were generated with ViewerLite version 5.0 (Accelrys Inc., San Diego, CA).

12. *For example, the synthesis of compound* **7**: To a solution of ethyl oxalyl chloride (0.400 mL, 3.48 mmol) in THF (20 mL) were added triethylamine ($Et_3N$) (0.480 mL, 3.48 mmol) and *p*-toluidine (373 mg, 3.48 mmol) with stirring at 0 °C. The reaction mixture was allowed to warm to room temperature, and then stirred for 6 h. After removal by filtration of the resulting salts, the filtrate was concentrated under reduced pressure. The residue was extracted with EtOAc (50 mL), and the extract was washed successively with brine (20 mL), 1 M HCl (20 mL × 2), brine (20 mL), saturated $NaHCO_3$ (20 mL × 2) and brine (20 mL × 3), then dried over $MgSO_4$. Concentration under reduced pressure gave the crude ethyl oxalamate, which was used without further purification. To a solution of the crude ethyl oxalamate (640 mg, 3.09 mmol) in THF (30 mL) were added aqueous 1 M NaOH (3.40 mL, 3.40 mmol), water (50 mL) and MeOH (20 mL) with stirring at 0 °C. The reaction mixture was allowed to warm to room temperature, and then stirred for 20 h. After the addition of aqueous 1 M HCl (5 mL), MeOH and THF were evaporated under reduced pressure. The residue was acidified to pH 2 with 1 M HCl, and extracted with EtOAc (50 mL × 2). The combined organic layer was washed with brine (20 mL × 3), and dried over $MgSO_4$. Concentration under reduced pressure gave the crude acid, which was used for the next reaction without further purification. To a solution of the above crude acid (514 mg, 2.87 mmol) in THF (10 mL) were added 1-hydoxybenzotriazole (484 mg, 3.16 mmol), 4-amino-2,2,6,6-tetramethylpiperidine (446 μL, 2.58 mmol), 1-ethyl-3-(3-dimethylaminopropyl)carbodiimide hydrochloride (606 mg, 3.16 mmol) and $Et_3N$ (0.439 mL, 3.16 mmol) with stirring at 0 °C. The reaction mixture was allowed to warm to room temperature, and then stirred for 20 h. After evaporation of THF, the residue was dissolved in $CHCl_3$ (50 mL). The mixture was washed with saturated $NaHCO_3$ (20 mL × 2) and brine (20 mL × 3), and dried over $MgSO_4$. Concentration under reduced pressure gave the crude crystalline mass. The usual work-up followed by recrystallization from EtOAc–*n*-hexane gave the title compound **7** (363 mg, 1.14 mmol, 39.8%) as colorless crystals, mp = 176 °C; $\delta_H$ (400 MHz; $CDCl_3$) 1.07 (1H, m, NH), 1.16 (6H, s, $CH_3$), 1.29 (6H, s, $CH_3$), 1.44 (2H, m, $CH_2$), 1.91 (1H, d, *J* 3.7, C*H*H), 1.94 (1H, d, *J* 3.7, CH*H*), 2.34 (3H, s, $CH_3$), 4.25 (1H, m, CH), 7.17 (2H, d, *J* 8.3, ArH), 7.33 (1H, m, NH), 7.50 (2H, d, *J* 8.4, ArH), 9.18 (1H, s, NH); HRMS (FAB), *m/z* calcd for $C_{18}H_{28}N_3O_2$ $(MH)^+$ 318.2182, found 318.2173.
13. McFarland, C.; Vicic, D. A.; Debnath, A. K. *Synthesis* **2006**, 807.
14. *The synthesis of compound* **12**: To a solution of $Et_3N$ (417 μL, 3.00 mmol) and 4-nitroaniline (138 mg, 1.00 mmol) in THF (1.3 mL) was added oxalyl dichloride (85.8 μL, 1.00 mmol) with stirring at 0 °C. After being stirred for 30 min at 0 °C, $Et_3N$ (167 μL, 1.20 mmol) and 4-amino-2,2,6,6-tetramethylpiperidine (156 μL, 0.90 mmol) were added. The reaction mixture was stirred for 6 h at 0 °C. After removal by filtration of the resulting salts, the filtrate was concentrated under reduced pressure. The residue was dissolved in $CHCl_3$ (20 mL), and the mixture was washed successively with brine (10 mL), saturated $NaHCO_3$ (10 mL × 2) and brine (10 mL × 3), and dried over $MgSO_4$. Concentration under reduced pressure followed by flash chromatography over silica gel with $CHCl_3$–MeOH (9:1) gave 42.4 mg (0.122 mmol, 13.5%) of the title compound **12** as colorless crystals, mp = 190 °C; $\delta_H$ (400 MHz; $CDCl_3$) 1.09 (1H, m, NH), 1.17 (6H, s, $CH_3$), 1.29 (6H, s, $CH_3$), 1.43 (2H, m, $CH_2$), 1.92 (1H, d, *J* 3.8, C*H*H), 1.95 (1H, d, *J* 3.8, CH*H*), 4.28 (1H, m, CH), 7.29 (1H, m, NH), 7.82 (2H, d, *J* 9.1, ArH), 8.28 (2H, d, *J* 9.1, ArH), 9.55 (1H, s, NH); HRMS (FAB), *m/z* calcd for $C_{17}H_{25}N_4O_4$ $(MH)^+$ 349.1876, found 349.1871.
15. Yoshimura, K.; Shibata, J.; Kimura, T.; Honda, A.; Maeda, Y.; Koito, A.; Murakami, T.; Mitsuya, H.; Matsushita, S. *AIDS* **2006**, *20*, 2065.
16. (a) Chapman, N. B.; Shorter, J. *Advances in Linear Free Energy Relationship*; Plenum Press: London, 1972; (b) Chapman, N. B.; Shorter, J. *Correlation Analysis in Chemistry*; Plenum Press: London, 1978; (c) Hansch, C.; Leo, A. J.; Hoekman, D. *Exploring QSAR, Hydrophobic, Electronic, and Steric Constants*; American Chemical Society: Washington, DC, 1995.
17. Taft, R. W. In *Steric Effects in Organic Chemistry*; Newman, M. S., Ed.; John Wiley: New York, 1956; p 556.
18. (a) Chou, T. C.; Talalay, P. *J. Biol. Chem.* **1977**, *252*, 6438; (b) Chou, T. C.; Hayball, M. P. *CalcuSyn*, 2nd ed.; Biosoft: Cambridge, UK, 1996.

# Remodeling of Dynamic Structures of HIV-1 Envelope Proteins Leads to Synthetic Antigen Molecules Inducing Neutralizing Antibodies

Toru Nakahara,[†] Wataru Nomura,*[,†] Kenji Ohba,[‡] Aki Ohya,[†] Tomohiro Tanaka,[†] Chie Hashimoto,[†] Tetsuo Narumi,[†] Tsutomu Murakami,[‡] Naoki Yamamoto,[‡] and Hirokazu Tamamura*[,†]

Department of Medicinal Chemistry, Institute of Biomaterials and Bioengineering, Tokyo Medical and Dental University, 2-3-10 Kandasurugadai, Chiyoda-ku, Tokyo 101-0062, Japan, and AIDS Research Center, National Institute of Infectious Diseases, 1-23-1 Toyama, Shinjuku-ku, Tokyo 162-8640, Japan. Received November 16, 2009; Revised Manuscript Received February 28, 2010

A synthetic antigen targeting membrane-fusion mechanism of HIV-1 has a newly designed template with C3-symmetric linkers mimicking N36 trimeric form. The antiserum produced by immunization of the N36 trimeric form antigen showed structural preference in binding to N36 trimer and stronger inhibitory activity against HIV-1 infection than the N36 monomer. Our results suggest an effective strategy of HIV vaccine design based on a relationship to the native structure of proteins involved in HIV fusion mechanisms.

## INTRODUCTION

Antibody-based therapy is one of the promising treatments for AIDS. In recent years, AIDS antibodies have been produced by immunization (*1*) and by de novo engineering of monoclonal antibodies (mAb) with molecular evolution tactics such as phage display (*2*). Despite enormous efforts, however, only a limited number of highly and broadly HIV-neutralizing human mAbs have been isolated and characterized. These antibodies include gp41 Abs, 2F5 (*3*–*6*) and 4E10 (*5*–*7*), and gp120 Abs, 2G12 (*8*) and b12 (*9*). gp41 is a transmembrane envelope glycoprotein, which is divided into an endodomain and an ectodomain by the transmembrane region; the latter contains a hydrophobic amino-terminal fusion peptide, followed by amino-terminal and carboxy-terminal leucine/isoleucine heptad repeat domains with helical structures (HR1 and HR2, respectively). In the membrane fusion process of HIV-1, these subunits form a "pre-bundle" complex. The HR1 and HR2 regions are termed the N-terminal helix (N36) and C-terminal helix (C34), respectively. These helices form a six-helical bundle consisting of a central parallel trimeric coiled-coil of N36 surrounded by C34 in an antiparallel hairpin fashion. In design of immunogens that elicit broadly neutralizing antibodies, a useful strategy is to produce molecules that mimic the natural trimer on the virion surface. Previous studies show that these molecules could be proteins expressed as a recombinant form or on the surface of particles such as pseudovirions or proteoliposomes (*10*–*12*). The X-ray crystallographic study of gp41 shows that the distances between any two residues at the N-terminus of N-region are almost equal at approximately 10 Å (Figure 1A). A chemically synthetic template could be useful in connection with the design of a peptidomimetic corresponding to the native structure of gp41. To date, several gp41 mimetics have been synthesized as inhibitors or antigens and subjected to inhibition or neutralization assays (*13*–*16*). However, the templates for assembly of these helical peptides contain branched peptide linkers, which are not exactly equivalent in length (*14*). The N-terminal peptides constrained by another threefold linker showed high affinity for C-terminal peptides, although its biological advantages have not been determined (*15*). The mimicry can be estimated using the broadly neutralizing mAbs; suitable mimetics will bind neutralizing mAbs efficiently, but they will bind non-neutralizing mAbs poorly. In the present study, we designed and synthesized a novel three-helical bundle mimetic, which corresponds to the trimeric form of N36. We investigated whether mice immunized with the equivalent trimeric form of N36 mimetic can produce antibodies with stronger binding affinity for N36 trimer than for N36 monomer. This approach demonstrates the possibility of producing structure-specific antibodies by immunization of synthetic antigens corresponding to the natural form of viral proteins.

## EXPERIMENTAL PROCEDURES

**Conjugation of N36REGC and the Template to Produce triN36e.** Compound **6** (100 μg, 0.174 μmol) and N36REGC (3.4 mg, 0.574 μmol) were dissolved in a mixture of 300 μL of 200 mM acetate buffer (pH 5.2) and 300 μL of TFE under a nitrogen atmosphere, then TCEP·HCl was added. The reaction was stirred for 72 h at room temperature and monitored by HPLC. The ligation product (triN36e) was separated as an HPLC peak and was characterized by ESI-TOF-MS, *m/z* calcd for $C_{690}H_{1160}N_{226}O_{201}S_3$ 15933.1, found 15933.8. The purification was performed by reverse phase HPLC (YMC-Pack ODS-A column, 10 × 250 mm). Elution was carried out with a 40–50% linear gradient of acetonitrile (0.1% TFA) over 50 min. Purified triN36e, obtained in 16% yield, was identified by ESI-TOF-MS. The detailed synthesis of peptides is described in the Supporting Information (SI).

**CD Spectra.** CD measurements were performed with a J-720 circular dichroism spectrolarimeter equipped with a thermoregulator (JASCO). The wavelength dependence of molar ellipticity [θ] was monitored at 25 °C from 190 to 250 nm. Peptides were dissolved in 20 mM acetate buffer (pH 4.0) containing 40% MeOH (*23*, *24*). The experimental helicity was calculated as reported previously (*17*–*19*).

**Immunization and Sample Collection.** Six-week-old male BALB/c mice were purchased from Sankyo Laboratory Service Corp. (Tokyo, Japan) and maintained under specific pathogen-free conditions in an animal facility. The experimental protocol was approved by the ethical review committee of Tokyo Medical and Dental University. Freund incomplete adjuvant and PBS

* To whom correspondence should be addressed. E-mail: nomura.mr@tmd.ac.jp; tamamura.mr@tmd.ac.jp. phone: +81-3-5280-8036, fax: +81-3-5280-8039.

† Tokyo Medical and Dental University.

‡ National Institute of Infectious Diseases.

10.1021/bc900502z 
Published on Web 04/01/2010